Title	Roles of neural communication between the brain and thoracic ganglia in the selection and regulation of the cricket escape behavior
Author(s)	Sato, Nodoka; Shidara, Hisashi; Kamo, Shunsuke; Ogawa, Hiroto
Citation	Journal of insect physiology, 139, 104381 https://doi.org/10.1016/j.jinsphys.2022.104381
Issue Date	2022-05
Doc URL	http://hdl.handle.net/2115/90157
Rights	© 2022. This manuscript version is made available under the CC-BY-NC-ND 4.0 license http://creativecommons.org/licenses/by-nc-nd/4.0/
Rights(URL)	http://creativecommons.org/licenses/by-nc-nd/4.0/
Type	article (author version)
File Information	J_Insect_Physiol_139_104381.pdf

Title

Roles of neural communication between the brain and thoracic ganglia in the selection and regulation of the cricket escape behavior

Author names and affiliations

Nodoka Sato[1], Hisashi Shidara[2], Shunsuke Kamo[1], Hiroto Ogawa[2]

[1] Graduate school of Life Science, Hokkaido University, Sapporo 060-0810, Japan

[2] Department of Biological Sciences, Faculty of Science, Hokkaido University, Sapporo 060-0810, Japan

Corresponding author

Hiroto Ogawa

E-mail address: hogawa@sci.hokudai.ac.jp

Abbreviations:

CX: central complex body
CPG: central pattern generator
PTG: prothoracic ganglion
MsTG: mesothoracic ganglion
MtTG: metathoracic ganglion
SEG: subesophageal ganglion
TAG: terminal abdominal ganglion
TG: thoracic ganglia
VNC: ventral nerve cord
4th AG: 4th abdominal ganglion

Graphical abstract

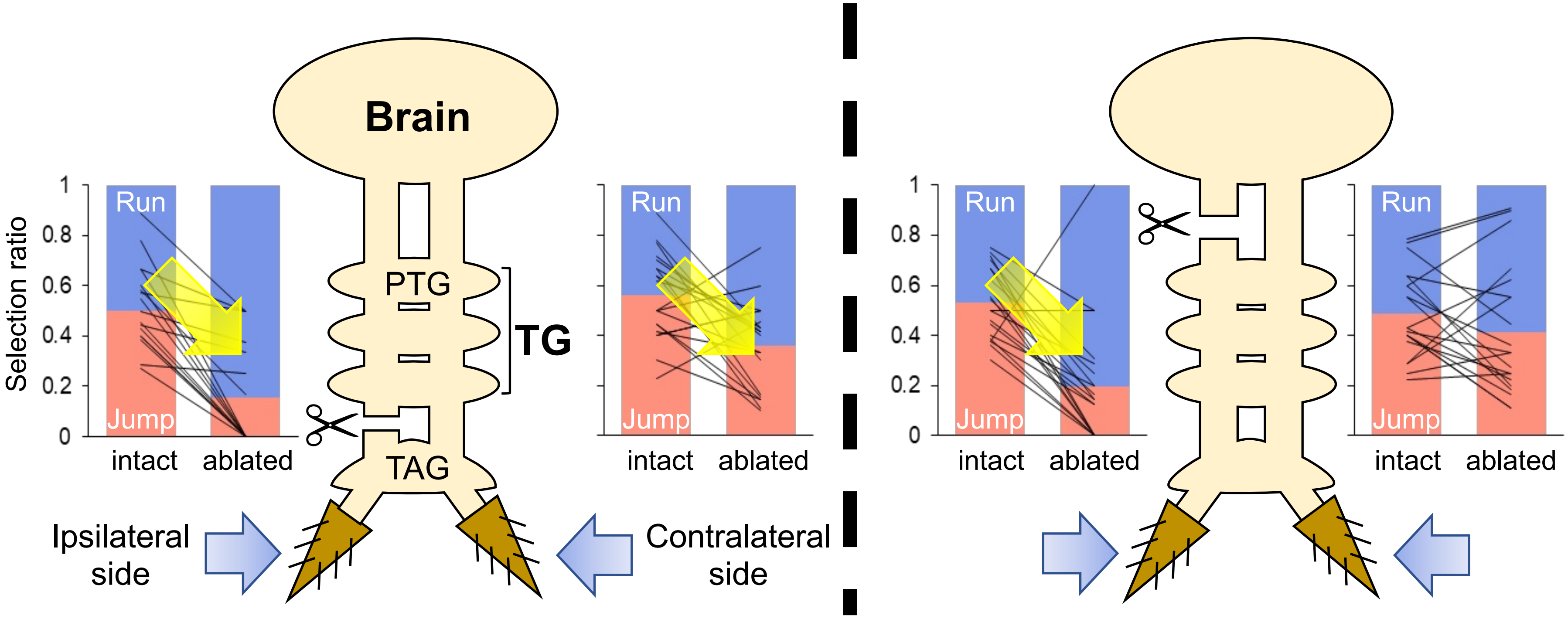

Highlights

- Ascending signals on ipsilateral side to stimulus is necessary for jumping escape.
- Hemi-lateral interaction between brain and thoracic ganglia allows running escape.
- Bilateral descending signals from the brain is important to regulate locomotion.
- Quick start to escape requires bilateral ascending signals to thoracis ganglia.
- Brain provides different descending signals before jumping and before running.

Abstract

To survive a predator's attack, prey animals must exhibit escape responses that are appropriately regulated in terms of their moving speed, distance, and direction. Insect locomotion is considered to be controlled by an interaction between the brain, which is involved in behavioral decision-making, and the thoracic ganglia (TG), which are primary motor centers. However, it remains unknown which descending and ascending signals between these neural centers are involved in the regulation of the escape behavior. We addressed the distinct roles of the brain and TG in the wind-elicited escape behavior of crickets by assessing the effects of partial ablation of the intersegmental communications on escape responses. We unilaterally cut the ventral nerve cord (VNC) at different locations, between the brain and TG, or between the TG and terminal abdominal ganglion (TAG), a primary sensory center of the cercal system. The partial ablation of ascending signals to the brain greatly reduced the jumping response rather than running, indicating that sensory information processing in the brain is essential for the choice of escape responses. The ablation of descending signals from the brain to the TG impaired locomotor performance and directional control of the escape responses, suggesting that locomotion in the escape behavior largely depends on the descending signals from the brain. Finally, the extracellular recording from the cervical VNC indicated a difference in the descending activities preceding the escape responses between running and jumping. Our results demonstrated that the brain sends the descending signals encoding the behavioral choice and locomotor regulation to the TG, while the TG seem to have other specific roles, such as in the preparation of escape movement.

Key words

Ascending signals, descending signals, escape behavior, decision-making, motor control, cercal system

1. Introduction

Animals, including insects, universally exhibit escape behaviors to survive predator attacks (Domenici et al., 2011a, b). Multiple types of escape responses accompanied by distinct movements have been observed in various animals species, resulting in differences in behavioral performance (Briggman et al., 2005; Kohashi and Oda, 2008; Liu and Hale, 2017; Sato et al., 2019). The prey animals immediately exhibit appropriate responses to the threat signal by rapidly converting the sensory signals, indicating the predator's approach to the motor outputs.

For quick input-to-output conversion for the escape response, insects employ a simple circuit consisting of small numbers of neurons (Card, 2012). The brain is considered a crucial center for providing descending command signals to the thoracic ganglia (TG), as the motor center, to perform the escape behavior. In flies, a pair of descending projection neurons identified as giant fibers directly activates thoracic motor neurons to move their legs and wings in response to a visual threatening stimulus (Allen et al., 2006; Fotowat et al., 2009; Hammond and O'Shea, 2007; Levine and Tracey, 1973; Trimarchi and Schneiderman, 1995). The activity of the giant fiber determines which of these two modes of escape responses the flies will choose: take-off with short or long latency (Card and Dickinson, 2008; von Reyn et al., 2014). This suggests that the descending signals include the command as outputs of the decision-making of the behavioral choice in the escape response.

In addition, the movement direction in the escape behavior is controlled by the descending signals from the brain. Recent studies of flies have shown that distinct descending neurons regulate the direction of spontaneous walking (Bidaye et al., 2014, 2020) and flying (Schnell et al., 2017). In cockroaches, the turning response to the mechanosensory stimulus of the antenna is also controlled by descending signals (Mu and Ritzmann, 2008; Ridgel et al., 2007). In the escape behavior, which is a typical 'oriented behavior', animals precisely move to the opposite side of the threat stimulus (Domenici et al., 2008; Sato et al., 2019); therefore, the descending signals from the brain likely play a crucial role in the control of the direction of escape.

The TG, which includes target neurons receiving descending signals, is considered as the motor center in locomotive behaviors. The central pattern generators (CPGs) network essential for the rhythmic movement of the legs during walking is also included in the TG (Borgmann et al., 2009). The thoracic interneurons coordinate motor neuron activities directly during jumping or flying in locusts (Burrows, 1980, 1992; Burrows and Siegler, 1978; Pearson and Robertson, 1981; Robertson et al., 1982). The descending signals from the brain to the TG are considered to play important roles in regulating locomotion, such as walking speed and direction (Bidaye et al., 2018). However, the overall function of the intersegmental circuitry between the brain and TG in the escape behavior remains unclear.

Crickets exhibit either running or jumping as an escape response to a short air current, indicating the predator's approach, which is mediated by the abdominal cercal sensory system (Casas and Dangles, 2010; Dupuy et al., 2011; Sato et al., 2017). An air current is detected by filiform hairs on the cerci (Landolfa and Miller, 1995; Shimozawa and Kanou, 1984), and the receptor neurons project their axons into the terminal abdominal ganglion (TAG) in a directionally orderly manner (Jacobs and Theunissen, 1996, 2000; Ogawa et al., 2006). Eight to ten pairs of ascending projection neurons identified as "giant interneurons" (GIs) receive excitatory synaptic inputs from the receptor neurons and encode the information of the air currents, such as velocity, direction, and frequency (Aldworth et al. 2011; Miller et al., 1991; Mulder-Rosi et al., 2010; Ogawa et al., 2008; Theunissen and Miller, 1991). Considering the previous report indicating direct and long axonal projections of GIs to the brain through the ventral nerve cord (VNC) (Hirota et al., 1993), the brain is considered to be the center of the crickets' wind-elicited escape behavior. We have reported that the crickets can regulate escape direction depending on the stimulus angle in jumping as precisely as in running (Sato et al., 2019). Thus, the brain is possibly responsible for the behavioral choice of either running or jumping and for the regulation of locomotion, based on the stimulus information. In our previous study, crickets could not regulate their movement direction in the running response to the air current after their unilateral VNC was ablated between the brain and TG, which also supports the importance of descending signals from the brain to control the escape direction (Oe and Ogawa, 2013).

In the present study, we elucidated the involvement of ascending/descending communication between the brain and TG in the wind-elicited escape behavior of crickets. We partly diminished the descending/ascending signals by cutting the unilateral VNC at two different locations and assessed its effects on behavioral choice and locomotor performance. The first was a cutting between the 4th abdominal ganglion (4th AG) and TAG, so that both the brain and TG received unilateral ascending signals and the TG received the paired descending signals from the brain as intact (Fig. 1A, left). The second was a cutting between subesophageal ganglion (SEG) and prothoracic ganglion (PTG), so that the ascending signals to the brain were ablated unilaterally as in the first cutting condition, while TG could receive intact ascending signals from TAG (Fig. 1A, right). Instead, the descending signals from the brain to the TG were eliminated on one side. Finally, in order to examine the differences in the descending command signals from the brain between running and jumping, we extracellularly recorded the descending signals that preceded the start of the escape behaviors.

2. Materials and methods

2.1. Animals

We used wild-type strains of crickets (*Gryllus bimaculatus*, Hokudai WT; Watanabe et al., 2018) that were bred in our laboratory. Throughout the experiments, 46 adult male crickets, less than 14 days after adult molting, were used. They were reared under 12-12 h light/dark conditions at a constant temperature of 27ºC. All experiments were conducted during the dark phase at 26–28°C.

2.2. Stimulation

The air-current stimulus was a short puff of nitrogen gas from a plastic nozzle (ø = 15 mm) connected to a pneumatic picopump (PV820, World Precision Instruments, Sarasota, FL, USA). One air-current nozzle was positioned on the same horizontal plane as the animal throughout the experiment. The velocity and duration of the air current were regulated as the injection pressure and opening or closing of the valve of the picopump.

2.3. Behavioral experiments

2.3.1. Experimental apparatus

Behavioral experiments were conducted using the same apparatus as in our previous study (Sato et al., 2019). We monitored the movement of the cricket in the wind-elicited escape responses using a high-speed digital camera (CH130EX, Shodensha, Osaka, Japan) installed above the circular arena (ø = 260 mm). The air-current nozzle was installed on the inside wall of the arena, and an air current of 834-mm/s velocity and 200-ms duration was used for all trials (Fig. 1B). The travel time of the air to the center was 14.6 ± 0.1 ms, which was measured as a delay in stimulus-evoked ascending spikes of projection neurons that were extracellularly recorded ($N = 2$ animals, 10 trials) at the center of the arena.

2.3.2. Procedure of the behavioral experiment

The basic procedure of the movement measurements in each trial was the same as in our previous study (Sato et al., 2019), which is described as follows. After being anesthetized by cooling with ice (0°C) for 10 min, crickets were marked with two white spots on the dorsal surface of the head and thorax, of which the size was large enough to detect the movement of crickets in images. The marked cricket was placed in the center of the arena within an inverted beaker (ø = 50 mm) covered with aluminum foil. After the beaker was carefully lifted up, an air-current stimulus was immediately applied to the cricket standing still, and the cricket's response was recorded by the camera. Since the crickets were oriented randomly within a beaker, the stimulus angles against the cricket varied across the trials. Based on the video data (shutter speed, 1 ms; sampling rate, 120 frames/s; total recording duration, 1660 ms), the two markers on the animal were automatically traced, and locomotor parameters that would be mentioned in a later section were measured using motion analysis software (Move-tr/2D, Library, Tokyo, Japan). To monitor the entire trajectory during movement, we adopted a 285.7 × 285.7 mm frame size with 1024 × 1024 pixels resolution, which covered the entire arena.

Two sessions of the behavioral experiment were performed for each animal: before ("intact" in figures) and after ("ablated" in figures) the VNC cutting (Fig. 1A). After more than 30 min of recovery from the anesthetization to mark the white spots, the first session of behavioral experiments was performed in the intact cricket. The crickets were then anesthetized again by cooling for 20 min for the VNC cutting treatment. For recovery, the treated crickets were left for 45 min or longer within a plastic container (138 mm × 220 mm × 135 mm) with free access to food and water. The second session of the experiment was performed after confirming recovery by visually checking that the crickets maintained the same posture and walked spontaneously as well as before the anesthetization. Twenty trials were repeated in each session at inter-trial intervals of 60–90 s. Therefore, 40 trials were performed for each individual.

2.3.3. VNC cutting

The VNC was severed using micro-scissors at either one of the following two locations: between the 4th AG and TAG, which was referred to as the 'abdomen-cut experiment' (Fig. 1B, left), or between SEG and PTG, referred to as the 'neck-cut experiment' (Fig. 1B, right). To sever the VNC, the anesthetized crickets were fixed on a silicon platform, ventral side up. For the neck-cut experiment, the epidermal membrane of the ventral surface of the cricket's neck was incised to expose the VNCs, and right or left VNC was unilaterally cut. For the abdomen-cut experiment, a small piece of the abdominal sternite was removed to expose the VNCs, and left or right VNC was unilaterally cut anterior to the TAG. After cutting, a piece of the sternite cuticle was placed on the incision. For each type of experiment, the right nerve was severed in 10 animals and the left nerve was severed in the remaining 10 animals; thus, a total of 20 animals were tested for each experiment. As a pre-confirmation experiment to check whether the connection between the brain and TG was essential for the escape behavior, the VNCs were bilaterally severed between SEG and PTG in five animals (Fig. S1A). For sham operations to check the just surgical effects except for VNC cutting, the epidermal membrane of the ventral surface of the cricket's neck or a small piece of the abdominal sternite was removed and returned without the VNC cutting (Figs. S3, S4).

2.3.4. Criteria of the wind-elicited escape response

The wind-elicited responses were analyzed in a manner similar to that in our previous study (Sato et al., 2017, 2019). Responses were considered as the first continuous movement (bout) and defined based on the translational velocity of the cricket movement. If the translational velocity exceeded 10 mm/s within 250 ms after the stimulus onset and was greater in its maximum value than 50 mm/s, the cricket was considered to “respond” to the stimulus. If the cricket did not begin to move within 250 ms of the response definition period, the trial was considered as “no response.” Then, the wind-elicited responses were categorized into “running” (Video S1) or “jumping” (Video S2) according to movement of the legs during the locomotion, which was determined visually for all the responding trials by checking the images frame by frame. If all six legs were off the ground simultaneously, the response was defined as “jumping.” If any one of the six legs touched the ground during movement, the response was defined as “running” (Fig. 1C). We rarely observed complex behaviors combined with running and jumping, such as jumping after running and *vice versa*. A third-party blind reviewer judged the responses either running or jumping using this criterion and obtained the same results as the experimenter.

2.3.5. Analysis of the behavioral data

The ‘all response probability’ was calculated as the ratio of all the responding trials, including running and jumping per total trials (20 trials) for each individual (Figs. 2, 3). In addition, the response probabilities for running or jumping were calculated as the ratio of the responses categorized as running or jumping per 20 trials for each individual. To assess the effects of the VNC cutting on the response probabilities, the difference in the response probabilities at intact and ablated conditions relative to the value at intact condition was calculated (Figs. 2G, 3G) as follows:

$$(Probability\ change) = (P_{ablated} - P_{intact})/P_{intact} \qquad (1)$$

where P_{intact} and $P_{ablated}$ are the probabilities at intact and ablated conditions, respectively. The selection ratio of running or jumping was calculated as the proportion between both responses for all responding trials for each individual and for all individuals (Figs. 2H, 3H).

Cricket movement during response was analyzed as in previous studies (Fukutomi et al., 2015; Oe and Ogawa, 2013; Sato et al., 2017, 2019). The response start was measured as the time when the translational velocity exceeded 10 mm/s after stimulus onset, and the response finish was measured as the time when the velocity was less than 10 mm/s. Movement distance, maximum translational velocity, and reaction time were measured as metric locomotor parameters that characterized escape movements (Figs. 4, 5). The movement distance was measured as the entire path length of the moving trajectory. The reaction time was calculated by subtracting the mean travel time of the air current, as mentioned above, from the delay of the valve opening of the picopump to the response start. To assess the effects of the VNC cutting on these metric locomotor parameters, the difference between the values at intact and ablated conditions relative to the value at intact condition was calculated (Fig. S2) as follows:

$$(Difference\ in\ parameter) = (M_{ablated} - M_{intact})/M_{intact} \qquad (2)$$

where M_{intact} and $M_{ablated}$ are the metric locomotor parameters at intact and ablated conditions, respectively. Angular parameters including movement direction and turn angle were calculated based on the cricket's body axis, which is a vector connecting the thoracic and head markers (Fig. 1D, center and right). The movement direction was measured as the angle between the body axis at the starting point of the response and a line connecting the thoracic markers at the start and finish points. The stimulus angle was defined as the angle between the downstream orientation of the air current and the body axis of the animal (Fig. 1D, left). Thus, if the cricket moved in the direction opposite to the stimulus source, the movement direction would be equal to the stimulus angle. The turn angle was measured as the angle between the body axes at the start and finish points of the initial response. If the cricket is oriented to the exact opposite side of the stimulus source at the finish points, the turn angle would be equal to the stimulus angle. As it has been confirmed in a previous study that crickets move in the opposite direction to the stimulus in both running and jumping (Sato et al., 2019), the absolute values of the difference between the movement direction and stimulus angle and that between the turn angle and movement direction were measured to assess the effects of VNC cutting on directional control in escape locomotion.

2.4. Extracellular recording of the descending signals

2.4.1. Electrophysiology

The descending neural activities evoked by the air-current stimulus were recorded extracellularly in head-fixed crickets (N = 6 animals, Fig. 8). Crickets were anesthetized for 1 h or longer by cooling with ice (0°C), and their antennae were removed. Then, their head and thorax were fixed dorsal side up with beeswax on a semi-cylindrical platform made of a 1.5-mL plastic tube. The VNCs were exposed, and the right VNC was severed between the SEG and PTG, where it was also cut in the neck-cut experiments. The treated cricket was held with the head-fixing platform connected to a magnetic stand and placed on a flexible stage. The flexible stage was made up of layers of the tracing paper to prevent cricket's legs from slipping and the plastic sheet on which crickets could keep their posture. This flexible stage was flexibly bent by the movements of the hind legs of the cricket so that the cricket could exhibit both running and jumping movements on it even in the head-fixed preparation. The descending signals were recorded extracellularly using a glass suction electrode placed on the distal cut end of the right VNC. The recorded signals were amplified by an analog amplifier (MEG-5200, Nihon Kohden, Tokyo, Japan), filtered with a bandpass of 150–3000 Hz, and digitized at 20 kHz through an A-D converter (Powerlab 4/26, ADInstruments, Bella Vista, NSW, Australia). In addition to the extracellular recording, the leg movements were monitored using a high-speed digital camera used for the behavioral experiments. Electrophysiological recording was started more than 1 h after the anesthetization was terminated. Descending activities were recorded in six animals.

For electrophysiological recording, an air-current stimulus of 618 or 734 mm/s velocity and 200-ms duration was used. The stimulus was applied through the nozzle that was placed on the same horizontal plane as the animal, at a distance of 100 mm from the left side (contralateral side to ablation) of the animal (Fig. 8A). This is because the results of the neck-cut experiments revealed that the crickets whose the VNC was unilaterally cut between SEG and PTG could even exhibit running and jumping in response to the stimulus from their contralateral side to ablation (Fig. 3). Ten trials of responses to air currents of either 618 or 734 mm/s velocity were recorded in each session of the experiment at inter-trial intervals of 60 s. Four sessions with these two different velocities of stimuli were performed for each individual in the order of the sessions was 618, 734, 618, and 734 mm/s of the stimulus velocities (Fig. 8D). Thus, 20 trials of responses were recorded for each stimulus velocity, and 40 trials were recorded for each individual. The crickets were allowed to rest for 5 min between different sessions in the head-fixed position.

2.4.2. Analysis of the behavioral responses

Unlike in the VNC cutting experiments, it was impossible to measure the locomotor parameters of the head-fixed cricket in the electrophysiological experiment. Thus, we determined the type of behavioral responses, which were classified into jumping, running, or no response, based on leg movement by checking the video images frame by frame. By using similar criteria for the behavioral experiments in the free-moving crickets, if any legs began to move within 250 ms after stimulus onset, the cricket was considered to respond to the stimulus. If both hind legs synchronously kicked the paper sheet in the initial response, the response was defined as "jumping." If the left and right hind legs moved alternatively instead of a synchronous kick, the response was defined as "running." Behavioral onset was defined as the time of the first frame when the animals began to move their legs.

2.4.3. Analysis of the electrophysiological data

To analyze the descending spikes, we used WaveClus software (Chaure et al., 2018). The recorded data were digitally filtered with a 300–3000 Hz band-pass, and spikes were detected with a threshold that was set to five times the standard deviation of the voltages throughout the recording. The firing rate was calculated as the spike counts for each time bin of 10-ms width. To align the time course of the firing rate to the onset of the behavioral response, the time of the response onset was subtracted from the time of the individual spike peaks, and then the spikes were counted in each 10-ms bin. The descending signals were compared in the following values between running and jumping responses: the first spike timing, total spike counts, spike counts preceding the movement onset, and maximum spike counts following the movement onset (Fig. 8G–J). The first spike timing was defined as the time of the first spike evoked after the stimulus onset. The total spike counts were measured as the number of all evoked spikes for two different periods: the period between the stimulus onset and movement onset (pre time) and the 1500-ms period after the movement onset (post time). The spike count preceding the behavioral onset was measured as the number of spikes evoked for a 10-ms period before the movement onset. The maximum spike count was measured as the peak value of the firing rates for each 10-ms time-bin that was moved at a resolution of 1 ms after the movement onset.

2.5. Statistical analysis

R programming software (ver. 3.6.2, R Development Core Team) was used for all statistical analyses.

2.5.1. Statistics for behavioral data

Due to the fact that the response probabilities were strongly affected by VNC cutting, the sample size of the data for the responding trials varied among the sessions (Table S1). Considering the varied sample sizes, a generalized linear mixed model (GLMM, the package 'glmmML' ver. 1.1.1 in R) was used to assess the effect of VNC cutting on the all-response probability and the selection ratio (Figs. 2D, 2H, 3D, 3H). The response probability and selection ratio in this model were assumed to be Poisson distributed. We assumed the GLMM with the following two parameters as the explanatory variables: the cutting condition that was either intact or ablated (cut) and the stimulated side that was either the contralateral or ipsilateral side to ablation ($side$), as follows:

$$(Response\ probability) = \beta_0 + \beta_1(cut) + \beta_2(side) + \beta_3(cut{:}\,side) + r \quad (3)$$

$$(Selection\ ratio) = \beta_0 + \beta_1(cut) + \beta_2(side) + \beta_3(cut{:}\,side) + r \quad (4)$$

To assess the effects of VNC cutting on the changes in response probabilities and locomotor parameters, which were confirmed to be Gaussian distributed, we used linear mixed-effects models (LMM, the package 'nlme' ver. 3.1-151 in R). For the probability changes (Figs. 2G, 3G), we assumed LMM with the type of response that was either running or jumping ($response$) and the stimulated side ($side$) as explanatory variables, as follows:

$$(Probability\ change) = \beta_0 + \beta_1(response) + \beta_2(side) + \beta_3(response{:}\,side) + r \quad (5)$$

To assess the effect of VNC cutting on the metric locomotor parameters (Figs. 4, 5), we assumed LMM with the effect of the type of response ($response$), cutting condition (cut), and stimulated side ($side$) as the explanatory variables, as follows:

$$(Parameter) = \beta_0 + \beta_1(response) + \beta_2(cut) + \beta_3(side) + \beta_4(response{:}\,cut) + \beta_5(response{:}\,side) + \beta_6(cut{:}\,side) + \beta_7(response{:}\,cut{:}\,side) + r \quad (6)$$

For the differences in locomotor parameters between intact and ablated conditions (Fig. S2), we assumed the LMM with the effect of the type of response ($response$), stimulated side ($side$), and cutting location that was either the abdomen or neck ($location$) as the explanatory variables, as follows:

$$(Difference\ in\ parameter) = \beta_0 + \beta_1(response) + \beta_2(side) + \beta_3(location) + \beta_4(response{:}\,side) + \beta_5(response{:}\,location) + \beta_6(side{:}\,location) +$$

$$\beta_7(response\colon side\colon location) + r \qquad (7)$$

In all of the GLMMs and LMMs, r is the random effect indicating the ID of the animal. The significance of the coefficients for each explanatory variable and their interactions (β) were used to assess their effects on the all-response probability or selection ratio (Tables S2–7).

As in previous studies (Oe and Ogawa, 2013; Sato et al., 2017), the movement direction was considered as non-circular data and linear regression analysis was used as follows:

$$(Movement\ direction) = a(stimulus\ angle) + b, \qquad (8)$$

where a is the estimated coefficient and b is the intercept. Furthermore, the relationship between the movement direction and turn angle was also examined using linear regression analysis, as follows:

$$(Turn\ angle) = a(movement\ direction) + b \qquad (9)$$

where a is the estimated coefficient and b is the intercept. The relationships between the angular parameters were assessed based on the significance of the coefficients (Table S8). To assess the effect of VNC cutting on directional control, the LMM (8) used for the metric locomotor parameters was adopted for the absolute difference between the movement direction and stimulus angle and that between the turn angle and movement direction. The significance of the coefficient for each explanatory variable and their interactions was used to assess the effects of the absolute differences between the angular parameters (Table S9).

2.5.2. Statistics for the electrophysiological data

In the analysis of descending signals, the sample size of running and jumping varied in six individuals (Table S10). Thus, the LMM (package ‘lme4’ ver. 1.1-23 in R) was adopted to compare the characteristics of the evoked spikes, such as the first spike timing and spike counts, between running and jumping. We assumed LMMs that included the response type, which was either jumping or running, as the explanatory variable, and animal IDs considered as random effects, as follows:

$$(Parameter\ in\ spiking\ response) = \beta_0 + \beta_1(response\ type) + r \qquad (10)$$

where r is a random effect. The significance of the effect of response type on the characteristics of the spiking response was tested by comparing the LMMs with and without the explanatory variables of response type using the likelihood ratio test (Table S11).

3. Results

3.1. Ablation of the ascending sensory signals diminished jumping response

To examine the contribution of the communication between the brain and TG in the wind-elicited escape behavior of crickets, we partially or fully ablated the ascending/descending signals by cutting the VNC. The bilateral severing of the VNCs between the SEG and PTG (Fig. S1A) completely abolished the escape response to the air current (Fig. S1B), indicating that the interaction between the brain and TG was essential for the escape behavior. The VNC was then unilaterally severed at two different locations (Fig. 1A), and its effect on action selection were tested.

First, the VNC was unilaterally cut between the 4th AG and the TAG. In this condition, half of the ascending signals to both the TG and the brain were ablated, but the descending signals were provided bilaterally from the brain to the TG (abdomen-cut experiment, Fig. 1B, left). The cutting of the VNC greatly reduced the jumping in response to the stimulus from any direction, but did not affect the running in response to the stimulus from the contralateral side to ablation (Fig. 2). As shown in Fig. 2A–C, the escape responses to the stimulus from the ipsilateral side were more largely decreased after VNC cutting than those to the stimulus from the contralateral side. The GLMM (see Material and method) indicated that the variable of “cut” and the interaction of “cut” and “$side$” variables had significant effects on the all-response probability (Fig. 2D, Table S4). This demonstrated that VNC cutting impaired the escape responses to the stimulus from any direction and that the impairment was greater for the ipsilateral side than for the contralateral side to ablation. In addition, jumping was reduced more than running on both stimulus sides (Fig. 2E, F). The LMM to test the changes in probabilities of running and jumping indicated a significant effect of the variable of “$response$” (Fig. 2G, Table

S5), meaning that the jumping probability was more decreased by the cutting than the running probability. The effect of the “$side$” variable on the changes in probabilities was also significant, thus both the running and jumping probabilities were more reduced for the ipsilateral side than for the contralateral side to ablation. The running response to the stimulus from the contralateral side was not reduced at ablated condition (Fig. 2B, E, G). The GLMM analysis for the choice of either running or jumping indicated the significant effects of the “cut” variable on the proportion of jumping per all responses (Fig. 2H, Table S4); thus, the crickets chose jumping less frequently after cutting regardless of the stimulated side. In addition, sham surgery of the abdominal VNC cutting had any influences neither the response probability nor selection ratio (Figs. S3A, S3B, Table S2), demonstrating that the changes in these parameters resulted solely from the unilateral VNC ablation. Thus, the results of the abdominal VNC cutting revealed that the escape responses to the air current were induced mainly by ascending sensory signals through the VNC ipsilateral to the stimulated side and that the jumping response to the stimulus from any direction required bilateral ascending signals.

Next, we unilaterally cut the VNC between the SEG and PTG (neck-cut experiment, Fig. 1B, right). In this case, half of the ascending sensory input to the brain was ablated in a manner similar to the abdomen-cut experiment, but that to the TGs was intact. Instead, the TG received only unilateral descending signals from the brain. Unilateral VNC-cutting at the neck abolished only the jumping response to the stimulus from the ipsilateral side to ablation of the crickets (Fig. 3). After the VNC cutting, the jumping was rarely elicited by the stimulus from the ipsilateral side, whereas running was unaffected on both sides (Fig. 3A–C). In the neck-cut experiment, the GLMM indicated the significant effects of the variable of “cut” and the interaction of “cut”and “$side$”

variables on the all-response probability (Fig. 3D, Table S4), meaning that VNC cutting reduced the probability more significantly for the ipsilateral side than for the contralateral side to ablation. In contrast to the results of the abdomen-cut experiment, only the probability of jumping in response to the stimulus from the ipsilateral side appeared to decrease (Fig. 3E–G). The LMM indicated the significant effect of only the interaction of "cut"and "$side$" variables on the changes in response probability (Fig. 3G, Table S5); thus, the jumping response to the stimulus from the ipsilateral side was impaired drastically, compared to the jumping elicited by the stimulus from the contralateral side and running responses. The GLMM analysis for the proportion of jumping in all response also indicated only the significant effect of the interaction of "cut"and "$side$" variables (Fig. 3H, Table S4), meaning that the proportion of jumping decreased only for the ablation side. The sham surgery of the cervical VNC cutting also had no impacts on the response probability and selection ratio (Fig. S4A, S4B, Table S3). Taken together with the results of the abdomen-cut experiment, it is suggested that ascending signals ipsilateral to the stimulated side need to reach the brain for a jumping response. In addition, it is likely that the running could be performed by unilateral descending signals if the ascending sensory inputs reached the TG bilaterally.

3.2. The effects of VNC cutting on locomotor parameters

To examine the roles of the interaction between the brain and TG in regulating locomotion in escape responses, we first assessed the effects of VNC cutting at different locations on the metric parameters, including the movement distance, velocity, and reaction time. The effects of the response type, VNC cutting, and the stimulated side on the metric locomotor parameters were examined using LMM. In the abdomen-cut experiment, VNC cutting reduced the distance and velocity and increased the reaction time in both running and jumping, and the effect was larger for the ipsilateral side than for the contralateral side to ablation (Fig. 4). The variable of “cut” and the interaction of “cut”and “$side$” variables had significant effects on all metric locomotor parameters (Fig. 4, Table S6). This demonstrated that these parameters were affected by cutting and the effects were larger for the ipsilateral side than that for the contralateral side to ablation. In contrast, VNC cutting at the neck drastically reduced the distance and velocity of both running and jumping on both sides, but had little effect on the reaction time, unlike the abdomen-cut experiment (Fig. 5). The variable of “cut” had significant effect on the distance (Fig. 5A, Table S6); thus, the decrement in the distance was not significantly different between the stimulus sides in both running and jumping. The variable of “*cut*” and the interaction of “cut” and “$response$” variables significantly affected the velocity, meaning that VNC cutting reduced both running and jumping velocities but the reduction in running was more drastic than that in jumping (Fig. 5B, Table S6). Only the interaction of “cut”and “$side$” variables had significant effect on the reaction time, suggesting that the reaction time in both running and jumping slightly increased only for the ipsilateral-side stimuli (Fig. 5C, Table S6). The effect of “$response$” variable was also significant on the distance and velocity in both the abdomen-cut and neck-cut experiments (Figs. 4, 5, Table S6). Thus, the crickets moved farther and faster in jumping than in running regardless of the VNC cutting or the stimulus side, which is consistent with our previous study (Sato et al., 2019).

Although both the VNC cuttings at either the abdomen or neck affected all the metric locomotor parameters, their effects differed between the cutting locations. VNC cutting at the neck reduced the distance and velocity more significantly than that at the abdomen, whereas the reaction time in the responses to the ipsilateral-side stimuli increased more by cutting at the abdomen than at the neck (Fig. S2). The locomotor parameters appeared to be more changed by cutting in running than in jumping, although the effect of the variable of “$response$” was not significant in the LMM analysis (Fig. S2, Table S7). The variable of “$location$” had a significant effect on the differences between intact and ablated conditions in the distance and velocity (Fig. S2A, B, Table S7); thus, cutting at the neck more greatly reduced these parameters than that at the abdomen. In contrast, the variable of “$side$” and the interaction of “$side$” and “$location$” variables significantly affected the difference in the reaction time (Fig. S2C, Table S7). This indicated that the reaction time was longer for the ipsilateral side than for the contralateral side to ablation regardless of the response type or the cutting location, and the cutting VNC at the abdomen increased the reaction time for the ipsilateral side more significantly than that at the neck.

In the sham surgery of the abdominal cutting, there was no significant changes in all these parameters (Fig. S3C-E, Table S2), while the sham surgery of the VNC cutting at the neck did not affect the velocity but slightly reduced the movement distance and increase the reaction time (Fig. S4C-E, Table S3). Considering these results of the sham surgeries, a part of the large effects on the distance by the cervical cutting might include the surgical damage. However, the reduction of the movement distance by the VNC cuttings was much greater than that by the sham surgery, suggesting that the communication between the cephalic and thoracic ganglia would be crucial for longer distance escape movement. In contrast, the changes in the reaction time by the VNC cutting at the neck was significant only for the ipsilateral side but as small as that by the sham surgery. Thus, the VNC- cutting at the neck likely had a very little impact on the reaction time, but it was much smaller than the abdominal cutting.

3.3. Directional control required the sensory information processing in the brain

We previously reported that crickets accurately control their movement direction according to the stimulus angle (Sato et al., 2019). In addition, the crickets tend to turn during the escape response such that they orient to the direction of movement at the end of the initial response. We also examined the effect of VNC cutting on the angular control in the escape behavior.

VNC cutting at the abdomen had little effect on the control of the movement direction, but impaired the control of the turn angle in the escape responses to the stimuli from the ipsilateral side to ablation (Fig. 6). The movement direction was correlated with the stimulus angle even at ablated condition, and the linear regression lines for the movement direction against the stimulus angle were close to the $y = x$ line in both running and jumping (Fig. 6A, Table S8). This indicated that the crickets moved in the opposite direction to the stimulus, as reported in our previous study (Sato et al., 2019). However, the relationship between the movement direction and turn angle was abolished by VNC cutting (Fig. 6B, Table S8). The turn angle was correlated with the direction of movement elicited by the stimulus from the contralateral side to ablation (Fig. 6B, > 0° of the movement direction). However, in the escape response to the stimulus from the ipsilateral side, most of the turn angles were distributed on the positive area. This indicated that the crickets were able to move to the opposite side of the stimulus source, but turned their body axis toward the stimulated side in response to the stimulus from the ipsilateral side. These changes in the relationship between the movement direction and turn angle was not observed in the sham surgery experiment (Fig. S3). To assess the accuracy of control in the movement direction and turn angle, we analyzed the absolute difference between the movement direction and stimulus angle, or between the turn angle and movement direction, using LMM. The interaction of “cut” and “$side$” variables had a significant effect on both differences (Fig. 6C, D, Table S9), indicating that VNC cutting at the abdomen impaired the control of the movement direction and turn angle in the escape responses to the stimuli from the ipsilateral side to ablation. In addition, a significant effect of the “cut” variable on the difference between the movement direction and stimulus angle suggested that abdominal VNC-cutting had an impact on the movement direction elicited by the stimuli from the contralateral side to ablation. The “$response$” variable significantly affected both differences, implying the difference in the directional control between running and jumping (Table S9).

VNC cutting at the neck caused more serious effects on the directional control of the escape responses. After VNC cutting, the crickets moved forward without turning during both running and jumping (Fig. 7). The distribution of the plot and histograms of the responses at ablated condition indicated that the movement direction was concentrated around 0º, meaning forward movement. The linear regression lines were close to the $y = x$ line (Fig. 7A, Table S8), but this might be because the crickets moved backward, indicated as ± 180°, in some responses to the stimuli from behind. However, in contrast to the movements at intact condition, lateral movements were rarely elicited during both running and jumping. The turn angles were also close to 0º independent of the movement direction at ablated condition, especially during running (Fig. 7B, Table S8), indicating that the crickets were not turning. In contrast, even after the sham surgery of the VNC cutting at the neck, the crickets exhibited turning movement (Fig. S4). The LLM analysis indicated that the variable of “cut” and the interaction of “cut,” “$response$,” and “$side$”

variables significantly affected the absolute difference between the movement direction and stimulus angle (Fig. 7C, Table S9). This meant that VNC cutting significantly diminished the control of the movement direction against the stimulus angle in the escape responses to the stimuli from any direction. Meanwhile, the angular difference in jumping elicited by the stimuli from the ipsilateral side was not significantly different between intact and ablated conditions. This is probably because the jumping responses occurred almost exclusively in response to stimuli from behind. In the LMM analysis of the difference between the turn angle and movement direction, only the “$response$” variable had a significant effect (Fig. 7D, Table S9). Thus, VNC cutting at the neck did not have a significant impact on the control of the turn angle against the movement direction, but this may be due to the concentrated distribution of data plots (Fig. 7B).

3.4. Descending signals from the brain in running and jumping.

The different impacts of VNC cutting in the neck on running and jumping probabilities suggested that the action selection of either running or jumping required sensory information processing in the brain. If the sensory processing in the brain is necessary to choose either running or jumping, the descending neural activities from the brain to TG would include the command signals of the action selection. Then, to check the difference in the descending commands between running and jumping, we electrophysiologically recorded the descending signals preceding the running and jumping movements, which were simultaneously monitored using a high-speed camera (Fig. 8A–D). The time course in the descending spikes indicated a quick increase in their firing rate and slow decline after its peak for both running and jumping responses (Fig. 8E). The firing rate after the peak was consistently higher for jumping than for running, whereas no clear difference in the rising phase just after the stimulus onset was observed between running and jumping (Figs. 8E, S5). However, if the spike timings were aligned with the behavioral onset in each response, we found that the firing rate began to increase slightly earlier for running than for jumping (Figs. 8F, S6).

Quantitative analyses of the temporal profile of the firing rate revealed that the descending activity preceding jumping was more quickly elevated immediately before the behavioral onset than that preceding running (Fig. 8G–J). For some parameters characterizing the descending activity, the significance between running and jumping was tested using the likelihood ratio test for LMMs (see Materials and methods). When the spike timings were aligned with the stimulus onset, no significant difference in the time for the first spikes was observed between running and jumping. However, when aligned with the behavioral onset, the first spikes were evoked significantly earlier for running than for jumping, which was consistent across all recorded individuals (Fig. 8G, Table S11). This means that the jumping started more quickly following the descending spikes than running. The total number of spikes evoked during the period from the stimulus onset to the behavioral onset was greater during running than during jumping (pre time in Fig. 8H, Table S11). This is likely because the descending spikes preceding running were evoked earlier relative to the start of movement than that preceding jumping. In contrast, the spike counts for 10 ms just before the behavioral onset were higher in jumping than in running (Fig. 8I, Table S11), indicating that the descending activity increased to a higher level just before the onset of jumping than that of running. Focusing on the neural activity during the response, the total spike count after the behavioral onset (post time in Fig. 8H) and the maximum value in the firing rate were greater during jumping than during running (Fig. 8J, Table S11). Thus, the brain provides more descending signals to the TG during movements for jumping than for running.

4. Discussion

4.1. Abdominal and cervical VNC-cutting experiments revealed the important roles of the neural communication between the brain and TG in the escape behavior

In the present study, we elucidated the roles of the neural communications between the brain and TG in the wind-elicited escape of cricket. Bilateral VNC cutting at neck completely diminished the escape behavior including both running and jumping, thus neural interaction between the brain and TG was essential for the escape behavior. To further examine the roles of ascending or descending signals, the half of VNC was ablated at different locations. The half ablation of the ascending inputs to the brain and TG by abdominal cutting reduced response probability of both running and jumping, whereas the half ablation of ascending and descending signals to/from the brain by cervical cutting reduced only jumping but not running. This result meant that running required bilateral ascending inputs to TG and that bilateral communication between the brain and TG were necessary for jumping. Considering that the TG includes primary motor center in insect, neural processing in the brain were crucial for the choice of either running or jumping in the escape responses. Especially, the neural circuits essential for jumping are likely located in the brain.

The unilateral ablation of VNC at the abdomen or neck also had different impacts on the regulation of the escape locomotion. The VNC cuttings at either location reduced the movement distance and velocity. This suggested that bilateral ascending inputs to the brain would be needed for the high performance of escape responses and that the brain provided the descending signals to regulate the distance and velocity during escape locomotion. In contrast, the elongation of the reaction time for the ipsilateral-side stimulus was larger in the abdomen-cut than in the neck-cut experiment. Therefore, the bilateral ascending signals to the TGs would be more important for the quick start of the response rather than the descending signals from the brain. The VNC cutting had different effects also on the directional control depending on the severed location. Even after unilateral cutting of the VNC at the abdomen, the escape movement could be controlled in the movement direction and turn angle as accurately as in the contralateral side to ablation. It was demonstrated that the crickets could move and turn accurately even if half of the ascending signals were ablated. However, the directional control of the escape responses to the stimuli from the ipsilateral side to ablation was seriously affected, especially for the turning movement, suggesting that the control of movement direction mainly required ascending signals on the ipsilateral side of the stimulus. In contrast, the crickets could move only either forward or backward without turning after unilateral cutting of the VNC at the neck. This result demonstrated that the bilateral descending signals from the brain to the TGs would provide essential motor information for directional control of the escape behavior.

4.2. Brain function in the behavioral choice and locomotor regulation in the escape behavior

The results of the VNC cutting experiments at different locations indicated that sensorimotor processing in the brain played crucial roles in the behavioral choice and regulating locomotion in the escape behavior, which requires fast movement to survive. The jumping response required the sensory signals to ascend to the brain through the VNC ipsilateral to the stimulated side, suggesting the brain function for the choice of jumping or running. In flies, the activity of the brain descending neurons with different thresholds determines either two modes of take-off responses to visual looming stimuli

(Card and Dickinson, 2008; von Reyn et al., 2014). The identified giant fiber neurons responsible for the short mode response with a short reaction time have a higher threshold of the stimulus size than other descending neurons for the long mode. Stimulus velocity is important for the behavioral choice in flies: if the looming-stimulus was fast enough to reach the threshold to excite the giant fiber before the long mode was driven by the other descending neurons, the short-mode take-off is induced (von Reyn et al., 2014). Our preliminary results in another study indicate that the faster and longer the air currents, the more frequently the crickets exhibit jumping escape (Sato et al., BioRxiv 2021.04.23.441064). Therefore, in crickets, it is possible that the neural circuits within the brain integrate various types of information about the sensory stimulus, and the specific descending neurons trigger either jumping or running.

Cervical VNC-cutting had a larger impact on the distance and velocity, especially in running, than abdominal cutting (Figs. 4, 5), which suggests that the descending signals would provide the essential motor command to the TG to allow the crickets to run farther and faster in the escape behavior. The crickets treated with cervical VNC-cutting moved exclusively forward without turning regardless of the stimulus angle, while abdominal cutting had no significant effects on the direction and turn angle in the escape movement stimulated on the contralateral side to ablation. This result that the brain implements the regulation of escape direction is consistent with our previous study using the treadmill system (Oe and Ogawa, 2013). The GIs, which are considered to be the most important ascending neurons for the cercal-mediated behaviors, project a thick and long axon within the VNC contralateral side of the GI cell body from TAG to the brain (Hirota et al., 1993), and have distinct sensitivity to the stimulus angle, based on which the crickets decide the escape direction (Miller et al., 1991; Ogawa et al., 2008). The sensory signals provided by GIs are transformed into motor commands encoded by the descending signals in the brain, which are necessary to control their movement direction in the escape behavior. In cockroaches, the neural activity of the central complex (CX) has been reported to control movement direction and turning during walking (Guo and Ritzmann, 2013; Martin et al., 2015). Although the postsynaptic circuits of GIs in the brain have not been identified, CX may be involved in the neural pathways involved in escape locomotion.

4.3. Independent function of thoracic local circuits from the brain

In addition to the crucial roles of the brain in wind-elicited escape behavior, our results indicated that TG was also involved in some aspects of escape behavior. The different impacts of VNC cuttings on the running probability, depending on the cutting location, indicated that the bilateral ascending signals to the TG might be more important for running than the intact descending signals from the brain. It is possible that the neural circuits located in the TG have an independent function such as preparatory muscle contraction for running and jumping from the brain. Furthermore, abdominal VNC-cutting elongated the reaction time, but cervical cutting did not. This indicated that the bilateral ascending inputs to the TG would be important for the quick start of the escape response. Thus, the thoracic local circuits reported previously (Kanou and Shimozawa, 1985) may contribute to the immediate start of escape response, while high-speed locomotion and precise control of the movement direction are executed by processing in the brain. Cercal GIs arborize axon-collaterals within all segmental ganglia, including the TG, on the way of the main axonal shaft (Hirota et al., 1993), suggesting direct synaptic contacts with the thoracic neurons (Kanou and Shimozawa, 1985), similar to cockroaches

(Casagrand and Ritzmann, 1991; Ritzmann and Camhi, 1978; Ritzmann and Pollack, 1978). It is possible that the local connections between GIs and thoracic interneurons are involved in preparative contractions of the leg muscles so that the cricket can start to move immediately after the thoracic circuits receive the descending command from the brain.

4.4. Difference in descending signals for running and jumping

The results of the VNC cutting experiments suggested that the descending signals from the brain included multiple commands for escaping, such as the type of escape response, locomotion speed, and movement direction. Extracellular recordings indicated that descending activity preceding the responses differed in some aspects between running and jumping, even for the identical stimulus. This demonstrates that the descending signals from the brain are considered to provide different commands for either running or jumping. More descending spikes started to be generated before running than before jumping. In contrast, the descending activity increased more sharply before the start of jumping, meaning that the descending command signals to jump were sent immediately before the cricket started jumping. In other words, the descending signals allow the cricket to start jumping more quickly than running, which is consistent with the shorter reaction time for jumping compared to running, as shown in our previous study (Sato et al., 2019). Once the response was started, the number of spikes was sustained at a higher level during jumping than during running. Previous studies have reported that the rhythmic motor patterns during walking are enabled by CPG in TG (Borgmann et al., 2009), but that regulation of the walking direction requires the descending signals from the brain to TG (Bidaye et al., 2018). Considering this, the thoracic local circuits including CPGs may be able to regulate running independently, once the running direction is initially commanded by the descending signals. On the other hand, it is likely that jumping requires more continuous descending signals to maintain posture during jumping and landing.

The key descending neurons that directly trigger the specific escape response have been identified in several species of animals, but those for the crickets' wind-elicited escape behavior have not yet been identified. In locusts, the kinematics and neural basis of escape jumping have been well studied. The descending contralateral movement detector neuron (DCMD) triggers locust's jumping by receiving the visual stimulus information from the lobula giant motion detector (LGMD) (Gabbiani et al., 1999; Hatsopoulos et al., 1995; Rind, 1984) and sending the command to leg motor neurons (Burrows and Rowell, 1973; Fotowat and Gabbiani, 2007; Fotowat et al., 2011; Simmons et al., 2010). Jumping in crickets may be triggered by the command signals provided by a few specific descending neurons, such as the DCMD.

However, our results also suggest that more complicated neural circuits trigger jumping in crickets. It is noteworthy that the movement direction was precisely controlled in not only running but also jumping in crickets, which has been shown in our present and previous studies (Sato et al., 2017, 2019). Therefore, escape jumping in crickets is likely more controllable and flexible than that in locusts in which animals escape exclusively in a forward direction (Santer et al., 2005). In addition, ablation of unilateral descending signals of DCMD by cutting the VNC in locusts, similar to our neck-cut experiment, has little effect on jumping, unlike our present results (Santer et al., 2008; Fotowat et al., 2011). The half ablation of ascending and descending signals to and from the brain drastically reduced the jumping and diminished the controllability of the movement direction in crickets, whereas the descending command of DCMD on just one side is sufficient to elicit jumping in locusts. It is likely that the speed and direction of cricket jumping are regulated by multiple descending neurons rather than by single command neurons.

Unfortunately, it was technically difficult to identify the spike units specific to jumping or running because the extracellularly recorded descending spikes were very high in their firing frequency and contained many compound spikes. In crickets, nearly 200 brain neurons have axons that descend into the VNC on one side (Staudacher, 1998), and some of these neurons respond to various modalities of sensory stimuli, including air currents (Staudacher, 2001). It remains unknown which descending neurons are responsible for commanding running or jumping and regulating locomotion speed and direction in escape behavior. Further physiological investigation of brain neurons during escape behavior will allow us to identify the descending neurons conveying the command signals.

CRediT authorship contribution statement

Nodoka Sato: conceptualization, methodology, validation, formal analysis, investigation, data curation, writing – original draft preparation, visualization, project administration, funding acquisition. **Hisashi Shidara:** conceptualization, methodology, writing – review and editing, project administration. **Shunsuke Kamo:** investigation. **Hiroto Ogawa:** conceptualization, methodology, writing – review and editing, supervision, project administration, funding acquisition.

Declaration of Competing Interest:

The authors declare no competing or financial interests.

Acknowledgements:

We thank Dr. Makoto Mizunami and Dr. Masayo Soma for their helpful advices. We also thank Mr. Kazuhide Kiuchi for blind judgment of the responses either running or jumping.

Funding:

This work was supported by funding from JSPS KAKENHI grant number 16H06544 and to N.S. from JSPS, Grant-in-Aid for JSPS Research Fellow 19J10862.

References

Aldworth, Z.N., Dimitrov, A.G., Cummins, G.I., Gedeon, T., Miller, J.P., 2011. Temporal encoding in a nervous system. PLoS Computational Biology, 7, e1002041

Allen, M.J., Godenschwege, T.A., Tanouye, M.A., Phelan, P., 2006. Making an escape: Development and function of the *Drosophila* giant fibre system. Seminars in Cell and Development Biology, 17, 31–41.

Bidaye, S.S., Bockemühl, T., Büschges, A., 2018. Six-legged walking in insects: how CPGs, peripheral feedback, and descending signals generate coordinated and adaptive motor rhythms. Journal of Neurophysiology, 119, 459–475.

Bidaye, S.S., Laturney, M., Chang, A.K., Liu, Y., Bockemühl, T., Büschges, A., Scott, T., 2020. Two brain pathways initiate distinct forward walking programs in *Drosophila*. Neuron, 108, 469–485.

Bidaye, S.S., Machacek, C., Wu, Y., Dickson, B.J., 2014. Neuronal control of *Drosophila* walking direction. Science, 344, 97–101.

Borgmann, A., Hooper, S.L., Büschges, A., 2009. Sensory feedback induced by front-leg stepping entrains the activity of central pattern generators in caudal segments of the stick insect walking system. Journal of Neuroscience, 29, 2972–2983.

Briggman, K.L., Abarbanel, H.D., Kristan, W.B., 2005. Optical imaging of neuronal populations during decision-making. Science, 307, 896–901.

Burrows, M., 1980. The control of sets of motoneurones by local interneurones in the locust. Journal of Physiology, 298, 213–233.

Burrows, M., 1992. Local circuits for the control of leg movements in an insect. Trends in Neurosciences, 15, 226–232.

Burrows, M., Rowell, C.H.F., 1973. Connections between descending visual interneurons and metathoracic motoneurons in the locust. Journal of Comparative Physiology, 85, 221−234.

Burrows, M., Siegler, M.V.S., 1978. Graded synaptic transmission between local interneurons and motor neurons in the metathoracic ganglion of the locust. Journal of Physiology, 285, 231−255.

Card, G.M., 2012. Escape behaviors in insects. Current Opinion in Neurobiology, 22, 180−186.

Card, G., Dickinson, M., 2008. Performance trade-offs in the flight initiation of *Drosophila*. Journal of Experimental Biology, 211, 341−353.

Casagrand, J.L., Ritzmann, R.E., 1991. Localization of ventral giant interneuron connections to the ventral median branch of thoracic interneurons in the cockroach. Journal of Neurobiology, 22, 643−658.

Casas, J., Dangles, O., 2010. Physical ecology of fluid flow sensing in arthropods. Annual Review of Entomology, 55, 505−520.

Chaure, F.J., Rey, H.G., Quiroga, R.Q., 2018. A novel and fully automatic spike-sorting implementation with variable number of features. Journal of Neurophysiology, 120, 1859−1871.

Domenici, P., Booth, D., Blagburn, J.M., Bacon, J.P., 2008. Cockroaches keep predators guessing by using preferred escape trajectories. Current Biology, 18, 1792−1796.

Domenici, P., Blagburn, J.H., Bacon, J.P., 2011a. Animal escapology I: theoretical issues and emerging trends in escape trajectories. Journal of Experimental Biology, 214, 2463−2473.

Domenici, P., Blagburn, J.M., Bacon, J.P., 2011b. Animal escapology II: escape trajectory case studies. Journal of Experimental Biology, 214, 2474−2494.

Dupuy, F., Casas, J., Body, M., Lazzari, C.R., 2011. Danger detection and escape behaviour in wood crickets. Journal of Insect Physiology, 57, 865−871.

Fotowat, H., Fayyazuddin, A., Bellen, H.J., Gabbiani, F., 2009. A novel neuronal pathway for visually guided escape in *Drosophila melanogaster*. Journal of Neurophysiology, 102, 875−885.

Fotowat, H., Gabbiani, F., 2007. Relationship between the phases of sensory and motor activity during a looming-evoked multistage escape behavior. Journal of Neuroscience, 27, 10047−10059.

Fotowat, H., Harrison, R.R., Gabbiani, F., 2011. Multiplexing of motor information in the discharge of a collision detecting neuron during escape behaviors. Neuron, 69, 147−158.

Fukutomi, M., Someya, M., Ogawa, H., 2015. Auditory modulation of wind-elicited walking behavior in the cricket *Gryllus bimaculatus.* Journal of Experimental Biology, 218, 3968−3977.

Gabbiani, F., Krapp, H.G., Laurent, G., 1999. Computation of object approach by a wide-field, motion-sensitive neuron. Journal of Neuroscience, 19, 1122−1141.

Guo, P., Ritzmann, R.E., 2013. Neural activity in the central complex of the cockroach brain is linked to turning behaviors. Journal of Experimental Biology, 216, 992−1002.

Hammond, S., O’Shea, M., 2007. Escape flight initiation in the fly. Journal of Comparative Physiology A, 193, 471−476.

Hatsopoulos, N., Gabbiani, F., Laurent, G., 1995. Elementary computation of object approach by a wide-field visual neuron. Science, 270, 1000−1003.

Hirota, K., Sonoda, Y., Baba, Y., Yamaguchi, T., 1993. Distinction in morphology and behavioral role between dorsal and ventral groups of cricket giant interneurons.

Zoological Science, 10, 705–709.

Jacobs, G.A., Theunissen, F.E., 1996. Functional organization of a neural map in the cricket cercal sensory system. Journal of Neuroscience, 16, 769–784.

Jacobs, G.A., Theunissen, F.E., 2000. Extraction of sensory parameters from a neural map by primary sensory interneurons. Journal of Neuroscience, 20, 2934–2943.

Kanou, M., Shimozawa, T., 1985. Responses of cricket leg motoneurons to air-current stimuli: velocity dependent inhibition and acceleration dependent excitation. Zoological Science, 2, 629–639.

Kohashi, T., Oda, Y., 2008. Initiation of Mauthner- or non-Mauthner-mediated fast escape evoked by different modes of sensory input. Journal of Neuroscience, 28, 10641–10653.

Landolfa, M., Miller, J.P., 1995. Stimulus/response properties of cricket cercal filiform hair receptors. Journal of Comparative Physiology A, 177, 749–757.

Levine, J., Tracey, D., 1973. Structure and function of the giant motorneuron of *Drosophila melanogaster*. Journal of Comparative Physiology, 87, 213–235.

Liu, Y.C., Hale, M.E., 2017. Local spinal cord circuits and bilateral Mauthner cell activity function together to drive alternative startle behaviors. Current Biology, 27, 697–704.

Martin, J.P., Guo, P., Mu, L., Harley, C.M., Ritzmann, R.E., 2015. Central-complex control of movement in the freely walking cockroach. Current Biology, 25, 2795–2803.

Miller, J.P., Jacobs, G.A., Theunissen, F.E., 1991. Representation of sensory information in the cricket cercal sensory system. I. Response properties of the primary interneurons. Journal of Neurophysiology, 66, 1680–1689.

Mu, L., Ritzmann, R.E., 2008. Interaction between descending input and thoracic reflexes for joint coordination in cockroach: I. Descending influence on thoracic sensory reflexes. Journal of Comparative Physiology A, 194, 283−298.

Mulder-Rosi, J., Cummins, G.I., Miller, J.P., 2010. The cricket cercal system implements delay-line processing. Journal of Neurophysiology, 103, 1823–1832.

Ogawa, H., Cummins, G.I., Jacobs, G.A., Miller, J.P., 2006. Visualization of ensemble activity patterns of mechanosensory afferents in the cricket cercal sensory system with calcium imaging. Journal of Neurobiology, 66, 293−307.

Ogawa, H., Cummins, G.I., Jacobs, G.A., Oka, K., 2008. Dendritic design implements algorithm for synaptic extraction of sensory information. Journal of Neuroscience, 28, 4592–4603.

Oe, M., Ogawa, H., 2013. Neural basis of stimulus-angle-dependent motor control of wind-elicited walking behavior in the cricket *Gryllus bimaculatus*. PLoS ONE, 8, e80184.

Pearson, K.G., Robertson, R.M., 1981. Interneurons coactivating hindleg flexor and extensor motoneurons in the locust. Journal of Comparative Physiology A, 144, 391−400.

Ridgel, A.L., Alexander, B.E., Ritzmann, R.E., 2007. Descending control of turning behavior in the cockroach, *Blaberus discoidalis*. Journal of Comparative Physiology A, 193, 385−402.

Rind, F.C., 1984. A chemical synapse between two motion detecting neurones in the locust brain. Journal of Experimental Biology, 110, 143−167.

Ritzmann, R.E., Camhi, J.M., 1978. Excitation of leg motor neurons by giant interneurons in the cockroach *Periplaneta Americana*. Journal of Comparative Physiology A, 125, 305−316.

Ritzmann, R.E., Pollack, A.J., 1978. Identification of thoracic interneurons that mediate giant interneuron-to-motor pathways in the cockroach. Journal of Comparative Physiology A, 159, 639–654.

Robertson, R.M., Pearson, K.G., Reichert, H., 1982. Flight interneurons in the locust and the origin of insect wings. Science, 217, 177–179.

Santer, R.D., Yamazaki, Y., Rind, F.C., Simmons, P.J., 2005. Motor activity and trajectory control during escape jumping in the locust *Locusta migratoria*. Journal of Comparative Physiology A, 191, 965–975.

Santer, R.D., Yamazaki, Y., Rind, F.C., Simmons, P.J., 2008. Preparing for escape: an examination of the role of the DCMD neuron in locust escape jumps. Journal of Comparative Physiology A, 194, 69–77.

Sato, N., Shidara, H., Ogawa, H., 2017. Post-molting development of wind-elicited escape behavior in the cricket. Journal of Insect Physiology, 103, 36–46.

Sato, N., Shidara, H., Ogawa, H., 2019. Trade-off between motor performance and behavioural flexibility in the action selection of cricket escape behaviour. Scientific Reports, 9, 18112.

Schnell, B., Ros, I.G., Dickinson, M.H., 2017. A descending neuron correlated with the rapid steering maneuvers of flying *Drosophila*. Current Biology, 27, 1200–1205.

Shimozawa, T., Kanou, M., 1984. Varieties of filiform hairs: range fractionation by sensory afferents and cercal interneurons of a cricket. Journal of Comparative Physiology A, 155, 485–493.

Simmons, P.J., Rind, F.C., Santer, R.D., 2010. Escapes with and without preparation: The neuroethology of visual startle in locusts. Journal of Insect Physiology, 56, 876–883.

Staudacher, E., 1998. Distribution and morphology of descending brain neurons in the cricket *Gryllus bimaculatus*. Cell and Tissue Research, 294, 187–202.

Staudacher, E.M., 2001. Sensory responses of descending brain neurons in the walking cricket, *Gryllus bimaculatus*. Journal of Comparative Physiology A, 187, 1−17.

Theunissen, F.E., Miller, J.P., 1991. Representation of sensory information in the cricket cercal sensory system II. Information theoretic calculation of system accuracy and optimal tuning curve widths of four primary inter-neurons. Journal of Neurophysiology, 66, 1690–1703.

Trimarchi, J.R., Schneiderman, A.M., 1995. Different neural pathways coordinate *Drosophila* flight initiations evoked by visual and olfactory stimuli. Journal of Experimental Biology, 198, 1099−1104.

von Reyn, C.R., Breads, P., Peek, M.Y., Zheng, G.Z., Williamson, W.R., Yee, A.L., Leonardo, A., Card, G.M., 2014. A spike-timing mechanism for action selection. Nature Neuroscience, 17, 962–970.

Watanabe, T., Ugajin, A., Aonuma, H., 2018. Immediate-early promoter-driven transgenic reporter system for neuroethological research in a hemimetabolous insect. eNeuro, 5.

Figure legends

Fig. 1. VNC cutting experiments at different locations. (A) Diagram showing the locations of the VNC cutting. VNC was unilaterally severed between the 4th AG and TAG in the abdomen-cut experiment (left) or between the SEG and PTG in the neck-cut experiment (right). **(B)** Temporal scheme of VNC cutting experiments. In the same individuals, behavioral experiments were performed for intact and ablated conditions. **(C)** Schematic diagrams of leg movements during running (left) and jumping (right). The running was defined as a movement in which the left and right legs moved alternately, and at least any three of the legs contacted on the ground. The jumping was defined as a movement in which both hind legs flexed before kicking the ground, and all six legs simultaneously left the ground. Filled circles indicate the current position of each tarsus and open circles indicate the previous position. Double circles with inner filled and outer open circles indicate that the tarsus position was not changed, meaning the leg did not move at that step. **(D)** Diagram showing definitions of stimulus angle (left), movement direction (center), and turn angle (right).

Fig. 2. Abdominal VNC-cutting reduced the probability of both running and jumping. (A–C) Distributions of the number of responding trials for all responses including running and jumping (A), for running response (B), and for jumping response (C) against the stimulus angle. Histograms represent the data for the range of every 20º of the stimulus angles. Black open bars indicate the data at intact condition, and colored ones indicate that at ablated condition. Red dotted squares indicate the angular range of the stimuli from the ipsilateral side to ablation. **(D–E)** Probabilities of all responses (D),

running (E) and jumping (F) at intact and ablated conditions. The data are divided into the responses to the stimuli from the ipsilateral side (enclosed by a red dotted square) and those to the stimuli from the contralateral side to ablation. Gray open circles connected with gray lines represent the response probability for each individual, and black filled circles represent the mean of the probabilities for all individuals. **(G)** Changes in the probabilities of running and jumping. Colored filled circles represent the probability change for each individual, and black open circles represent the mean of the changes in probabilities for all individuals. **(H)** Selection ratio of the running (blue) and jumping (red) in all trials responding to the stimuli from the ipsilateral (enclosed by a red dotted square) or contralateral side to ablation. Black lines connect the proportion of the jumping responses per all responding trials for each individual. *N* = 20 animals.

Fig. 3. Cervical VNC-cutting reduced the probability of jumping but not of running. **(A–C)** Distributions of the number of responding trials for all responses including running and jumping (A), for running response (B), and for jumping response (C) against the stimulus angle. Histograms represent the data for the range of every 20º of the stimulus angles. Black open bars indicate the data at intact condition and colored ones indicate that at ablated condition. Red dotted squares indicate the angular range of the stimuli from the ipsilateral side to ablation. **(D–E)** Probabilities of all responses (D), running (E), and jumping (F) at intact and ablated conditions. The data are divided into the responses to the stimuli from the ipsilateral side (enclosed by a red dotted square) and those to the stimuli from the contralateral side to ablation. Gray open circles connected with gray lines represent the response probability for each individual, and black filled circles represent the mean of the probabilities for all individuals. **(G)** Changes in the probabilities of

running and jumping. Colored filled circles represent the probability changes for each individual, and black open circles represent the mean of the changes in probabilities for all individuals. **(H)** Selection ratio of the running (blue) and jumping (red) in all trials responding to the stimuli from the ipsilateral (enclosed by a red dotted square) or contralateral side to ablation. Black lines connect the proportion of the jumping responses per all responding trials for each individual. *N* = 20 animals.

Fig. 4. Abdominal VNC-cutting affected the locomotion parameters more largely in escape response to the stimuli from ipsilateral side to ablation. (A–C) Movement distance (A), maximum translational velocity (B), and reaction time (C) at intact and ablated conditions. The data are divided into the responses to the stimuli from the ipsilateral side (enclosed by a red dotted square) and those to the stimuli from the contralateral side to ablation. Colored bars indicate the mean value of data in all responding trials of running (blue) or jumping (red). Black open circles connected with lines indicate the mean value of data for each individual. *N* = 20 animals.

Fig. 5. Cervical VNC-cutting reduced the distance and velocity but did not affect the reaction times. (A–C) Movement distance (A), maximum translational velocity (B), and reaction time (C) at intact and ablated conditions. The data are divided into the responses to the stimuli from the ipsilateral side (enclosed by a red dotted square) and those to the stimuli from the contralateral side to ablation. Colored bars indicate the mean value of data in all responding trials of running (blue) or jumping (red). Black open circles connected with lines indicate the mean value of data for each individual. *N* = 20 animals.

Fig. 6. Abdominal VNC-cutting reduced the accuracy of the directional control in escape response to the stimuli from ipsilateral side to ablation. (A,B) Relationships between the movement direction and stimulus angle (A) and those between the turn angle and movement direction (B) at intact (left) and ablated conditions (right) in running (blue) and jumping (red). Colored lines represent linear regression lines for which significant correlation was observed, and black dotted lines represent $y = x$ lines. Histograms show the distributions of the data plotted against stimulus angle (above) or against movement direction (right side) in (A), and against movement direction (above) or against turn angle (right side) in (B), respectively. Red dotted square in (A) indicates the angular range of the stimuli from the ipsilateral side to ablation. **(C,D)** The absolute values of the difference between the movement direction and stimulus angle (C) and between the turn angle and movement direction (D) at intact and ablated conditions. The data are divided into the responses to the stimuli from the ipsilateral side (enclosed by a red dotted square) and those to the stimuli from the contralateral side to ablation. Colored bars indicate the mean value of data in all responding trials of running (blue) or jumping (red). Black open circles connected with lines indicate the mean value of data for each individual. $N = 20$ animals.

Fig. 7. Crickets escaped forward exclusively without turn after cervical VNC-cutting. (A,B) Relationships between the movement direction and stimulus angle (A) and those between the turn angle and movement direction (B) at intact (left) and ablated conditions (right) in running (blue) and jumping (red). Colored lines represent linear regression lines for which significant correlation was observed, and black dotted lines represent $y = x$ lines. Histograms show the distributions of the data plotted against stimulus angle (above)

or against movement direction (right side) in (A), and against movement direction (above) or against turn angle (right side) in (B), respectively. Red dotted square in (A) indicates the angular range of the stimuli from the ipsilateral side to ablation. **(C,D)** The absolute value of the difference between the movement direction and stimulus angle (C) and between the turn angle and movement direction (D) at intact and ablated conditions. The data are divided into the responses to the stimuli from the ipsilateral side (enclosed by a red dotted square) and those to the stimuli from the contralateral side to ablation. Colored bars indicate the mean value of data in all responding trials of running (blue) or jumping (red). Black open circles connected with lines indicate the mean value of data for each individual. $N = 20$ animals.

Fig. 8. Brain provided different descending signals before jumping from those before running. (A) Diagram showing the simultaneous recording of descending neural activities and cricket's movement. The cricket's head and thorax were fixed with a semi-cylindrical tube and placed on the paper sheet so that the cricket could move its legs freely. Air-current stimulus was applied from the contralateral side of the recorded VNC. The movement of cricket's legs was monitored with a high-speed camera from behind. **(B)** Diagram showing the extracellular recording of the descending activities using a suction electrode from the distal cut-end of right VNC between SEG and PTG. **(C)** Typical firing responses of descending activities in running (top) and jumping (bottom), which were recorded from the same individual. Lower traces indicate the air-current stimulus, of which the onset was marked by black arrowheads. **(D)** Temporal scheme of the experiment. Ten trials of one kind of stimulus were performed in each session, and 4 sessions were performed in the order of 618, 734, 618, and 734 mm/s of the stimulus

velocities. **(E,F)** Typical time course in firing rate aligned with stimulus onset (E) or behavioral onset (F), which were recorded from the same individual. The colored lines indicate mean of the number of spikes for each 10-ms time-bin in all responding trials of running (blue) and jumping (red) and the light-colored areas above and below the lines represent the range of ± SEM. Black bar in (E) indicates the stimulation, of which the onset was indicated as 0 on the time axes. Black dotted line in (F) indicates the behavioral onset indicated as 0 on the time axes. **(G)** Time of the first evoked spikes relative to the stimulus onset (left) or to the behavioral onset (right) in running (blue) and jumping (red). **(H)** Total numbers of spikes evoked before (left) or after (right) the start of running (blue) and jumping (red). Black filled circles represent the mean value of data in all responding trials. Colored plots represent the data for each responding trials. **(I,J)** The number of spikes evoked during 10 ms just before the start of movement (I) and the maximum value of the spike counts for each 10-ms bin after the start of movement (J). Colored bars indicate the mean of data in all responding trials of running (blue) and jumping (red). Black lines in (G), (H), (I), and (J) connect the mean values of the data for each individual. *$P < 0.05$, **$P < 0.01$, ***$P < 0.001$, likelihood ratio test for LMMs. $N = 6$ animals.

Fig 1

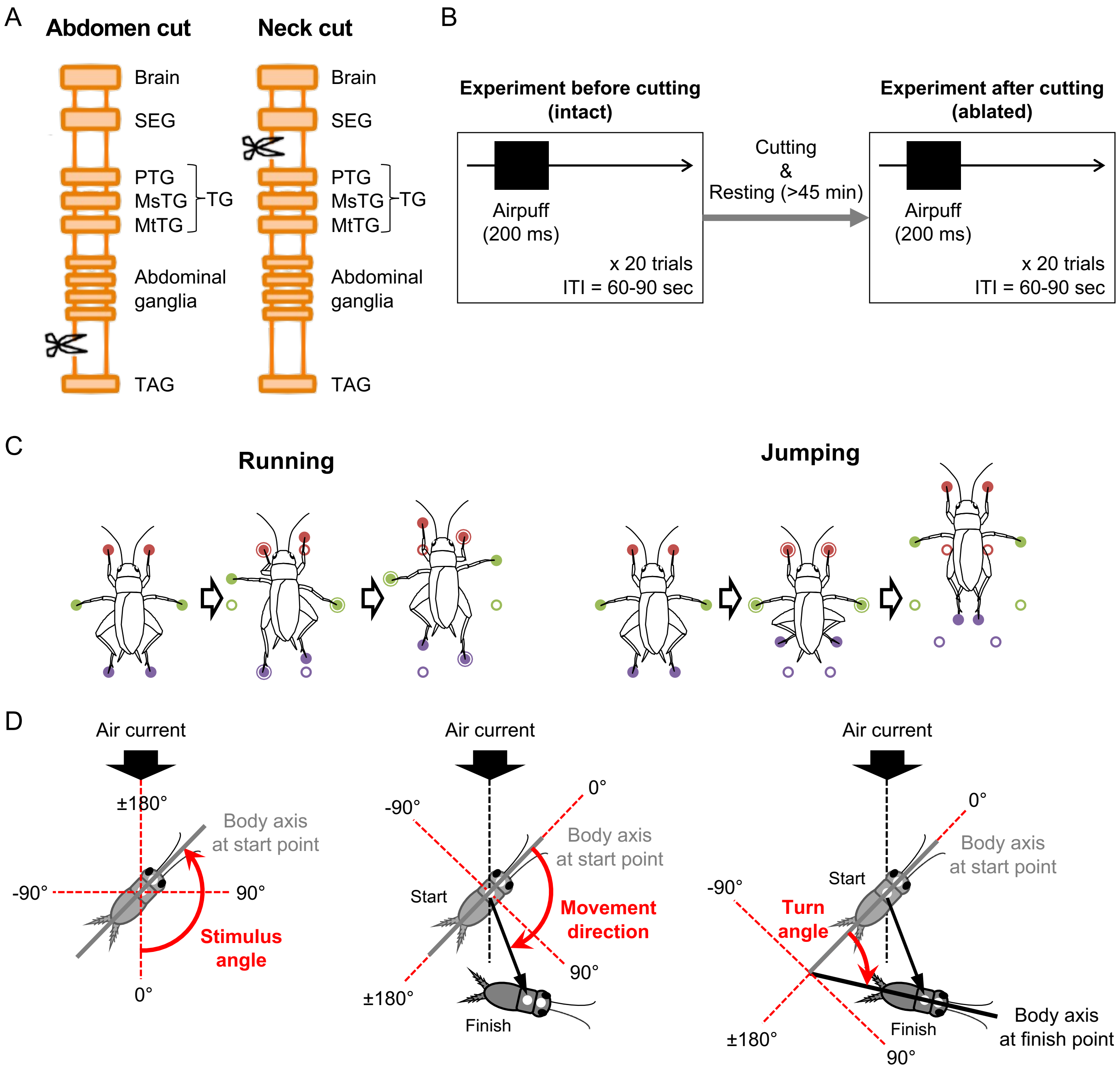
A
Abdomen cut
Brain
SEG
PTG
MsTG
MtTG
TG
Abdominal ganglia
TAG
Neck cut
Brain
SEG
PTG
MsTG
MtTG
TG
Abdominal ganglia
TAG
B
Experiment before cutting (intact)
Airpuff (200 ms)
x 20 trials
ITI = 60-90 sec
Cutting & Resting (>45 min)
Experiment after cutting (ablated)
Airpuff (200 ms)
x 20 trials
ITI = 60-90 sec
C
Running
Jumping
D
Air current
±180°
Body axis at start point
-90°
90°
Stimulus angle
0°
Air current
0°
-90°
Body axis at start point
Start
Movement direction
90°
±180°
Finish
Air current
0°
Body axis at start point
-90°
Start
Turn angle
Finish
Body axis at finish point
±180°
90°

Fig 2

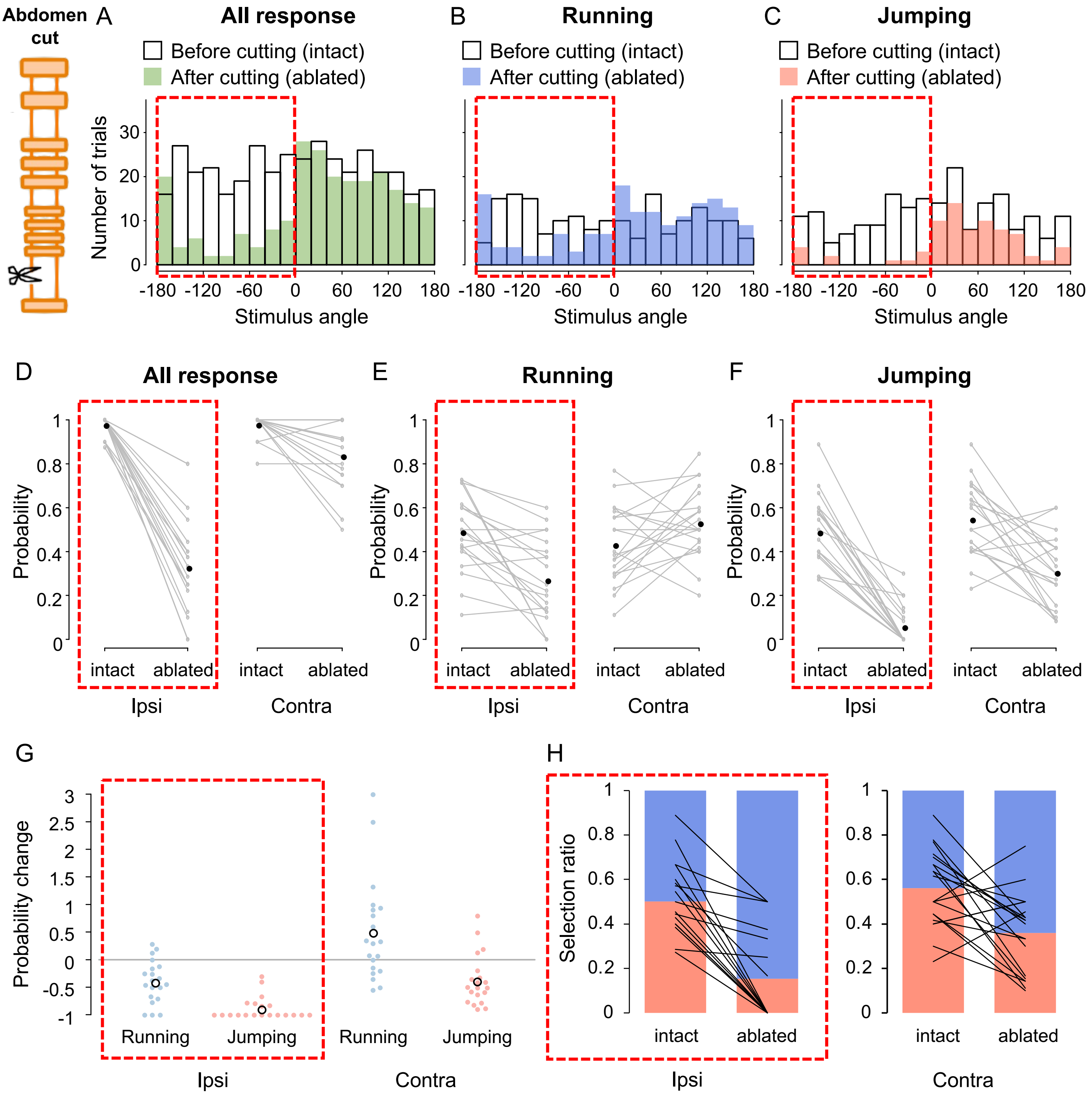
Abdomen cut
A
All response
☐ Before cutting (intact)
🟩 After cutting (ablated)
Number of trials
0
10
20
30
-180 -120 -60 0 60 120 180
Stimulus angle
B
Running
☐ Before cutting (intact)
🟦 After cutting (ablated)
-180 -120 -60 0 60 120 180
Stimulus angle
C
Jumping
☐ Before cutting (intact)
🟥 After cutting (ablated)
-180 -120 -60 0 60 120 180
Stimulus angle
D
All response
Probability
0
0.2
0.4
0.6
0.8
1
intact
ablated
intact
ablated
Ipsi
Contra
E
Running
Probability
0
0.2
0.4
0.6
0.8
1
intact
ablated
intact
ablated
Ipsi
Contra
F
Jumping
Probability
0
0.2
0.4
0.6
0.8
1
intact
ablated
intact
ablated
Ipsi
Contra
G
Probability change
-1
-0.5
0
0.5
1
1.5
2
2.5
3
Running
Jumping
Running
Jumping
Ipsi
Contra
H
Selection ratio
0
0.2
0.4
0.6
0.8
1
intact
ablated
Ipsi
0
0.2
0.4
0.6
0.8
1
intact
ablated
Contra

Fig 3

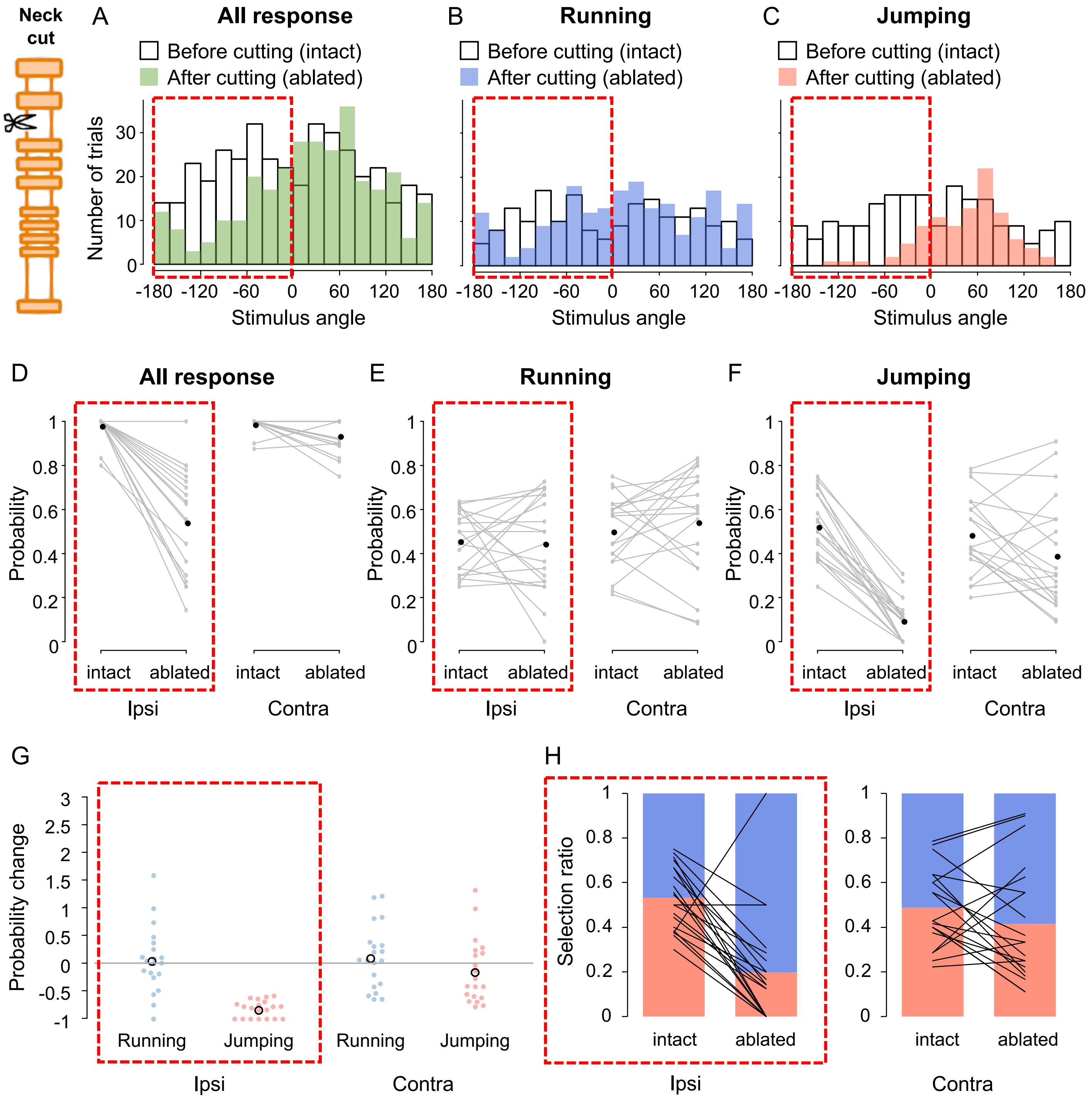
Neck cut
A
All response
Before cutting (intact)
After cutting (ablated)
Number of trials
Stimulus angle
-180 -120 -60 0 60 120 180
B
Running
Before cutting (intact)
After cutting (ablated)
Stimulus angle
C
Jumping
Before cutting (intact)
After cutting (ablated)
Stimulus angle
D
All response
E
Running
F
Jumping
Probability
intact
ablated
Ipsi
Contra
G
Probability change
Running
Jumping
Ipsi
Contra
H
Selection ratio
intact
ablated
Ipsi
Contra

Fig 4

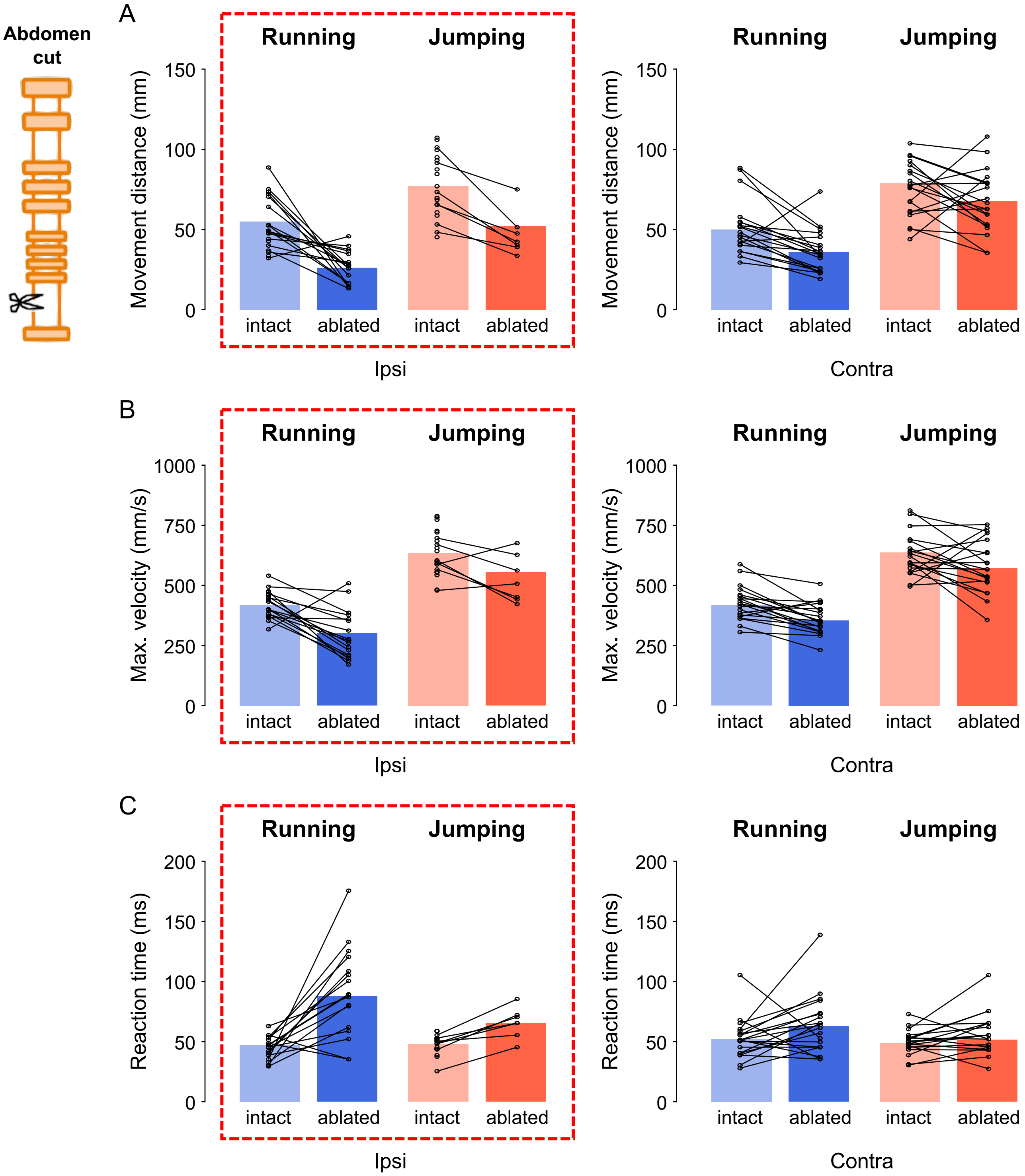
Abdomen cut
A
Running
Jumping
Movement distance (mm)
150
100
50
0
intact
ablated
intact
ablated
Ipsi
Contra
B
Max. velocity (mm/s)
1000
750
500
250
0
C
Reaction time (ms)
200
150
100
50
0

Fig 5

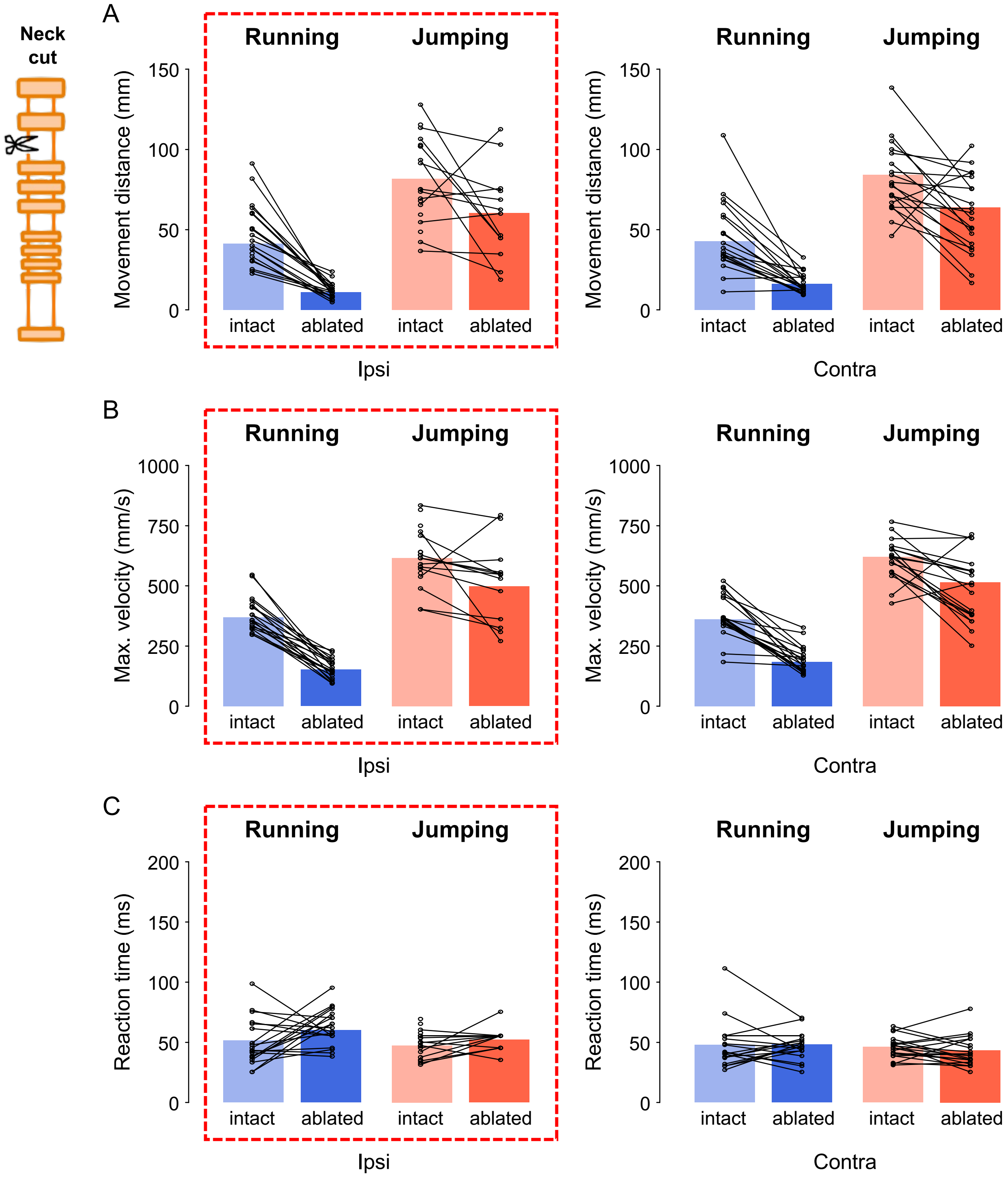
Neck cut
A
Running
Jumping
Movement distance (mm)
150
100
50
0
intact
ablated
intact
ablated
Ipsi
Running
Jumping
Movement distance (mm)
150
100
50
0
intact
ablated
intact
ablated
Contra
B
Running
Jumping
Max. velocity (mm/s)
1000
750
500
250
0
intact
ablated
intact
ablated
Ipsi
Running
Jumping
Max. velocity (mm/s)
1000
750
500
250
0
intact
ablated
intact
ablated
Contra
C
Running
Jumping
Reaction time (ms)
200
150
100
50
0
intact
ablated
intact
ablated
Ipsi
Running
Jumping
Reaction time (ms)
200
150
100
50
0
intact
ablated
intact
ablated
Contra

Fig 6

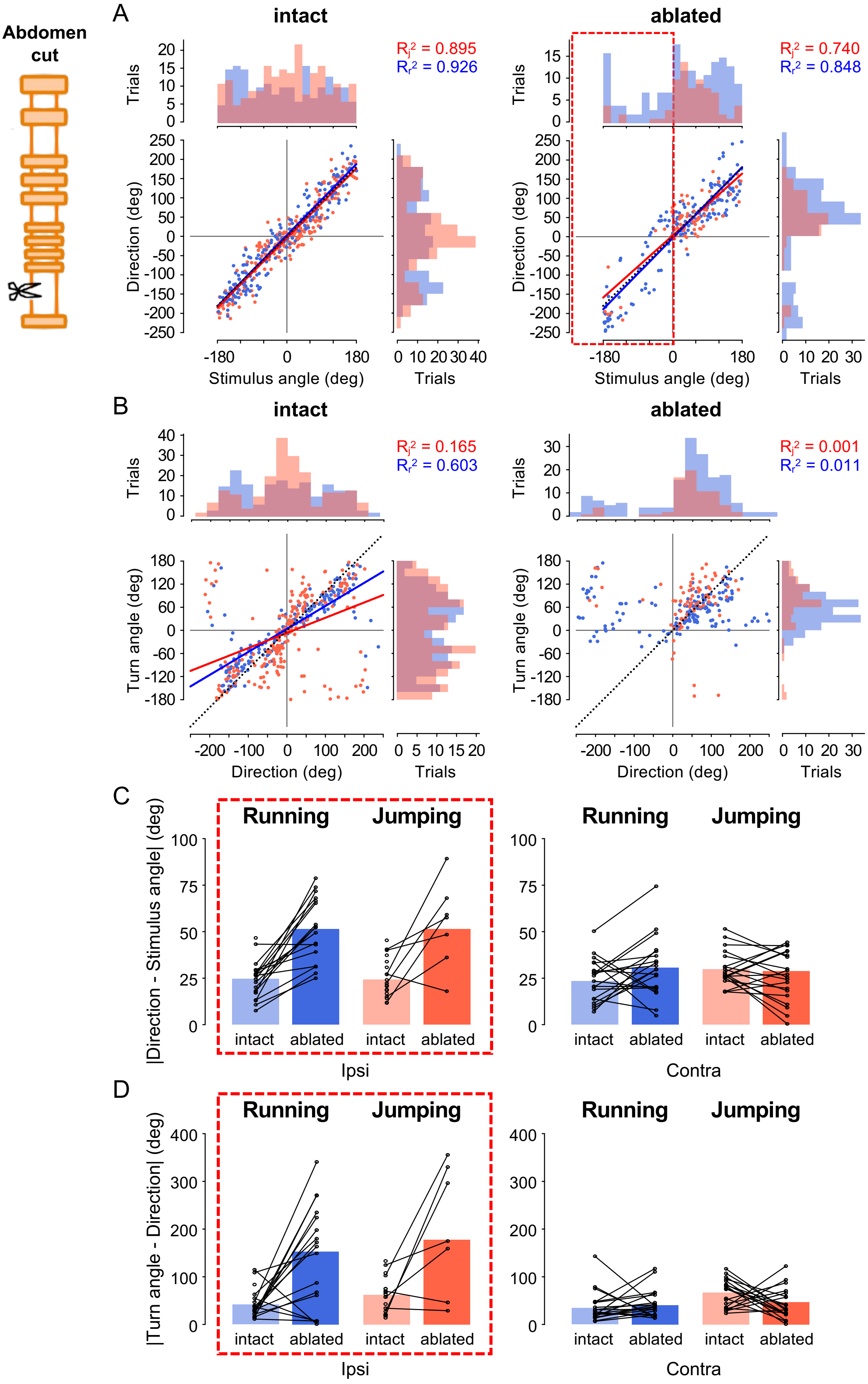
Abdomen cut
A
intact
ablated
$R_j^2 = 0.895$
$R_r^2 = 0.926$
$R_j^2 = 0.740$
$R_r^2 = 0.848$
Trials
Direction (deg)
Stimulus angle (deg)
-180
0
180
0 10 20 30 40
0 10 20 30
Trials
B
intact
ablated
$R_j^2 = 0.165$
$R_r^2 = 0.603$
$R_j^2 = 0.001$
$R_r^2 = 0.011$
Trials
Turn angle (deg)
Direction (deg)
-200 -100 0 100 200
0 5 10 15 20
0 10 20 30
Trials
C
Running
Jumping
Running
Jumping
|Direction - Stimulus angle| (deg)
0
25
50
75
100
intact
ablated
intact
ablated
Ipsi
Contra
D
Running
Jumping
Running
Jumping
|Turn angle - Direction| (deg)
0
100
200
300
400
intact
ablated
intact
ablated
Ipsi
Contra

Fig 7

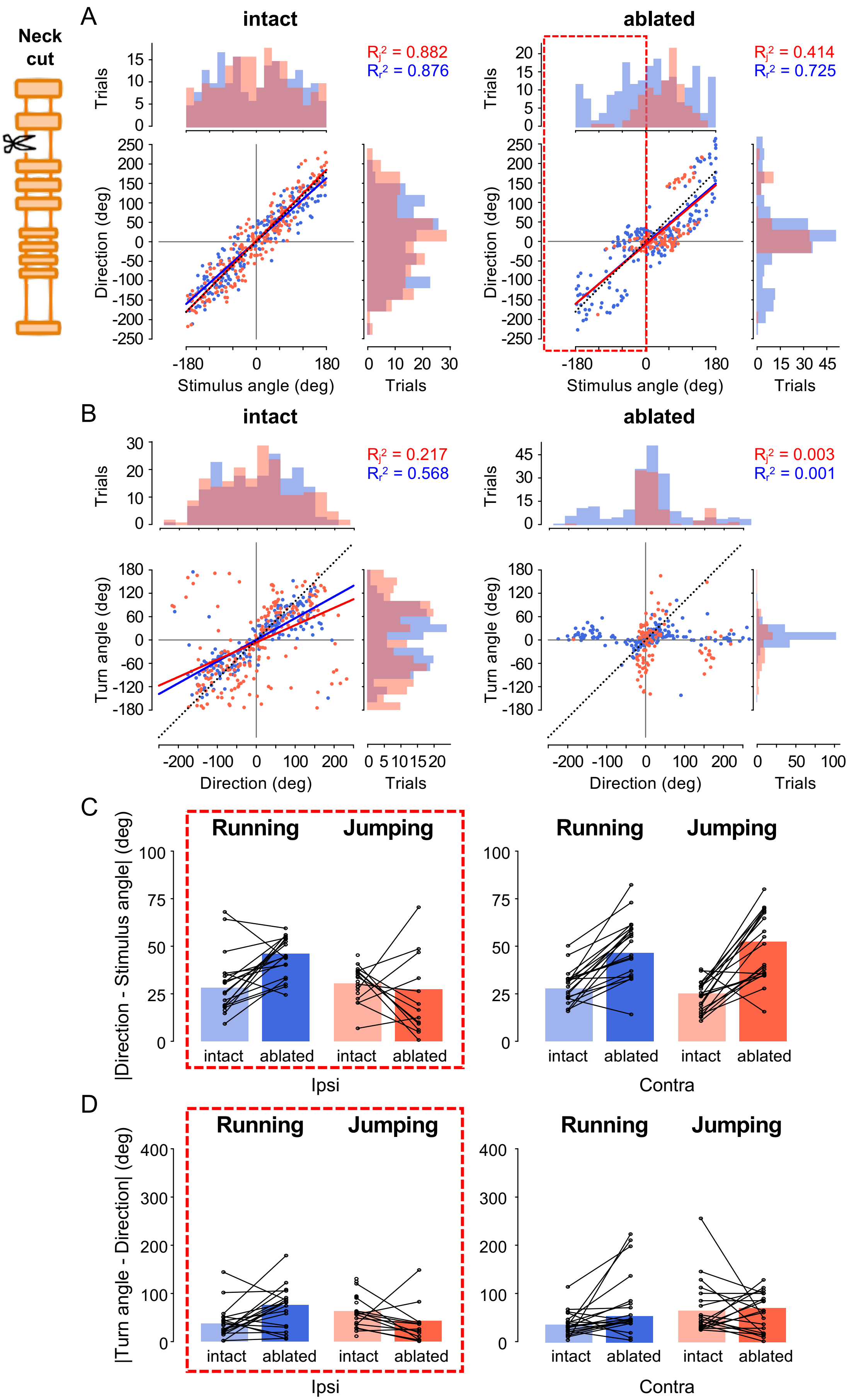
Neck cut
A
intact
ablated
Trials
R_j^2 = 0.882
R_r^2 = 0.876
R_j^2 = 0.414
R_r^2 = 0.725
Direction (deg)
Stimulus angle (deg)
Trials
B
intact
ablated
R_j^2 = 0.217
R_r^2 = 0.568
R_j^2 = 0.003
R_r^2 = 0.001
Turn angle (deg)
Direction (deg)
Trials
C
|Direction - Stimulus angle| (deg)
Running
Jumping
intact
ablated
intact
ablated
Ipsi
Contra
D
|Turn angle - Direction| (deg)
Running
Jumping
intact
ablated
intact
ablated
Ipsi
Contra

Fig 8

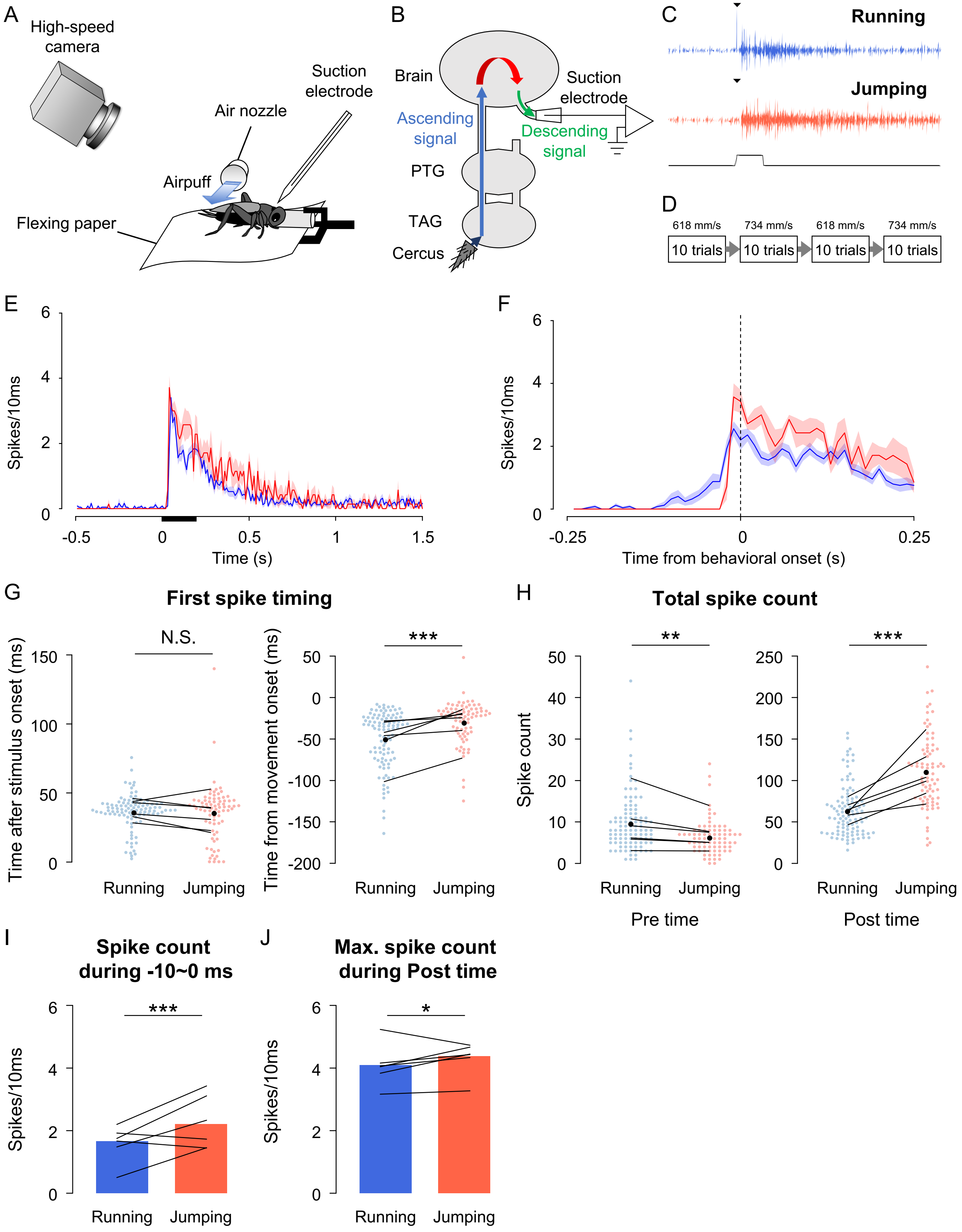
A
High-speed camera
Suction electrode
Air nozzle
Airpuff
Flexing paper
B
Brain
Suction electrode
Ascending signal
Descending signal
PTG
TAG
Cercus
C
Running
Jumping
D
618 mm/s
734 mm/s
618 mm/s
734 mm/s
10 trials
10 trials
10 trials
10 trials
E
Spikes/10ms
Time (s)
F
Spikes/10ms
Time from behavioral onset (s)
G
First spike timing
N.S.
Time after stimulus onset (ms)
***
Time from movement onset (ms)
Running
Jumping
H
Total spike count
**
***
Spike count
Running
Jumping
Pre time
Post time
I
Spike count during -10~0 ms
***
Spikes/10ms
Running
Jumping
J
Max. spike count during Post time
*
Spikes/10ms
Running
Jumping

Supplementary materials

Roles of neural communication between the brain and thoracic ganglia in the selection and regulation of the cricket escape behavior

Nodoka Sato, Hisashi Shidara, Hiroto Ogawa

Supplementary figures

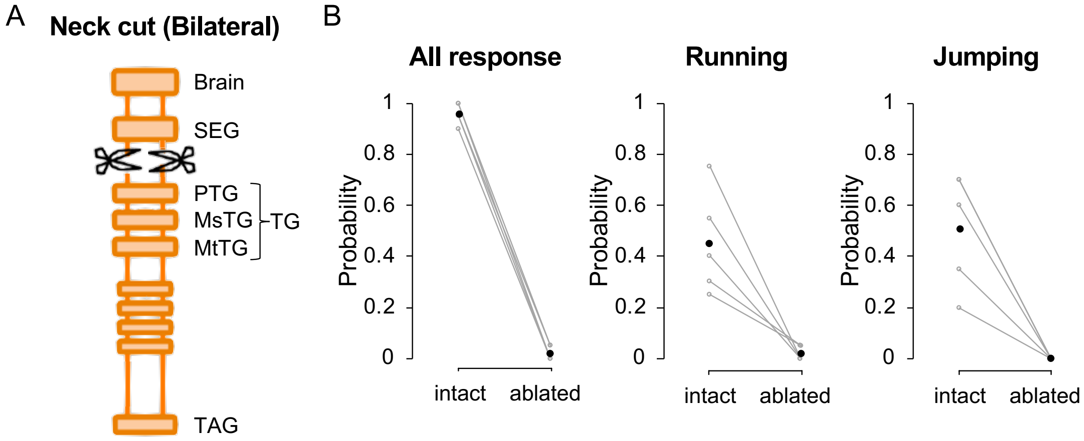

Fig. S1. Bilateral VNC-cutting at the neck completely abolished wind-elicited escape response. (A) Diagram showing the bilateral neck-cut experiment. The VNCs on both sides were severed at the neck between the SEG and PTG. **(B)** Response probabilities of all responses (left), running (middle), and jumping (right) before and after bilateral VNC cutting at the neck. Gray open circles connected with gray lines represent the response probability for each individual, and the black filled circles represent the mean of the probabilities for all individuals.

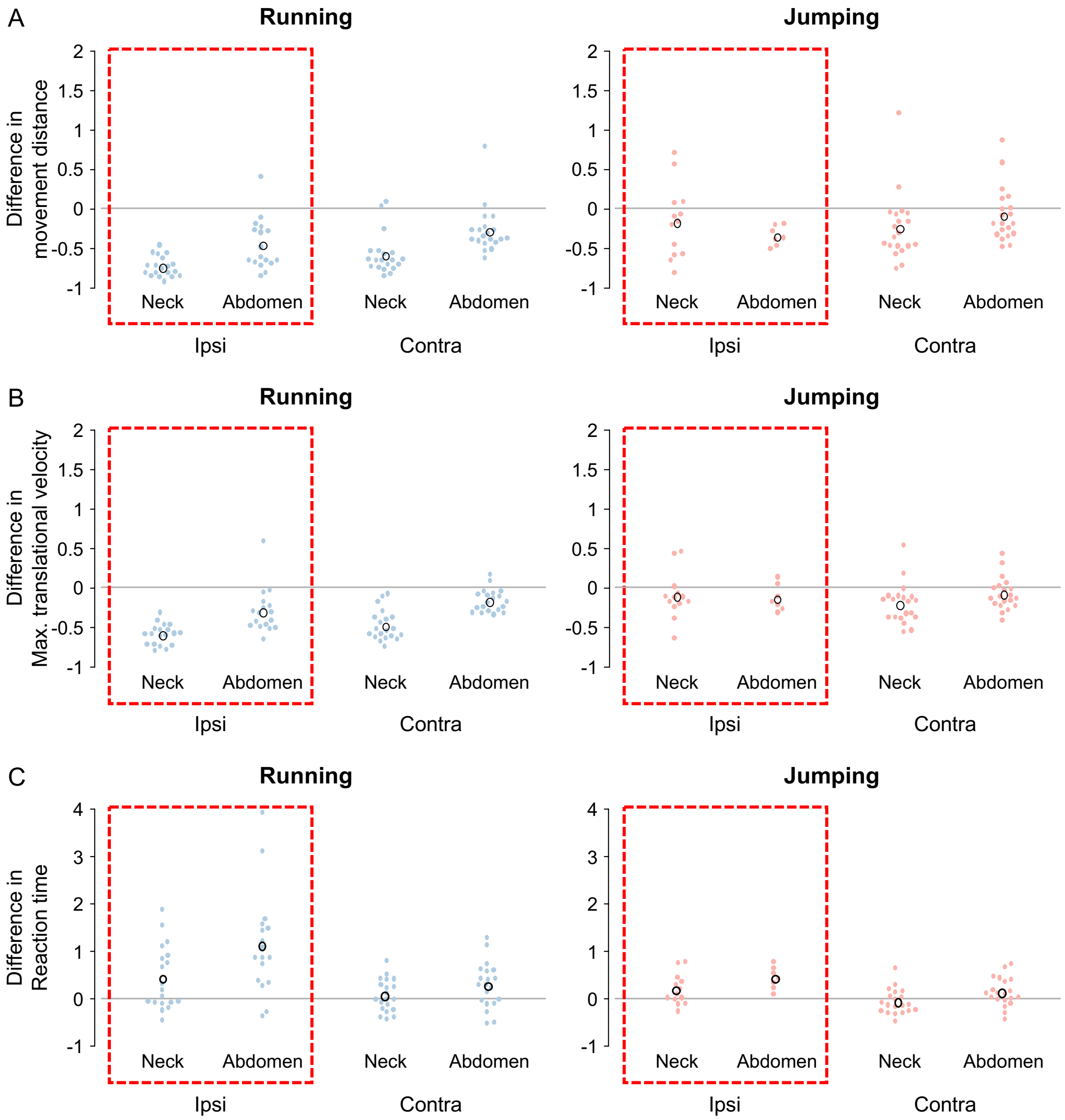

Fig. S2. Abdominal and cervical VNC-cutting had different effects on the locomotion in escape response. (A–C) Differences in the movement distance (A), maximum translational velocity (B), and reaction time (C) between intact and ablated conditions relative to those at intact condition. The data were divided into responses to the stimuli from the ipsilateral side (enclosed by a red dotted square) and responses to stimuli from the contralateral side to ablation. Colored filled circles represent the differences in mean values of differences in running (blue) and jumping (red) for each individual, and black open circles represent the mean of differences in all individuals. LMM for (A) indicated significant effects of “$location$” ($P = 0.003$), but not of any other explanatory variables ($P = 0.054$ for “$response$”, $P = 0.093$ for “$side$”, for, $P = 0.634$ for the interaction of “$response$” and “$side$”, $P = 0.322$ for the interaction of “$response$” and “$location$”, $P = 0.866$ for the interaction of “$side$” and “$location$”, $P = 0.186$ for the interaction of “$response$”, “$side$” and “$location$”). LMM for (B) indicated significant effects of “$location$” ($P < 0.001$), but not of any other explanatory variables ($P = 0.201$ for “$response$”, $P = 0.068$ for “$side$”, $P = 0.506$ for the interaction of “$response$” and “$side$”, $P = 0.057$ for the interaction of “$response$” and “$location$”, $P = 0.887$ for the interaction of “$side$” and “$location$”, $P = 0.371$ for the interaction of “$response$”, “$side$” and “$location$”). LMM for (C) indicated significant effects of “$side$” ($P < 0.001$) and the interaction of “$side$” and “$location$” ($P = 0.042$), but not of “$response$” ($P = 0.393$), “$location$” ($P = 0.200$), the interaction of “$response$” and “$side$” ($P = 0.085$), the interaction of “$response$” and “$location$” ($P = 0.961$), or the interaction of “$response$”, “$side$” and “$location$” ($P = 0.311$). $N = 20$ animals.

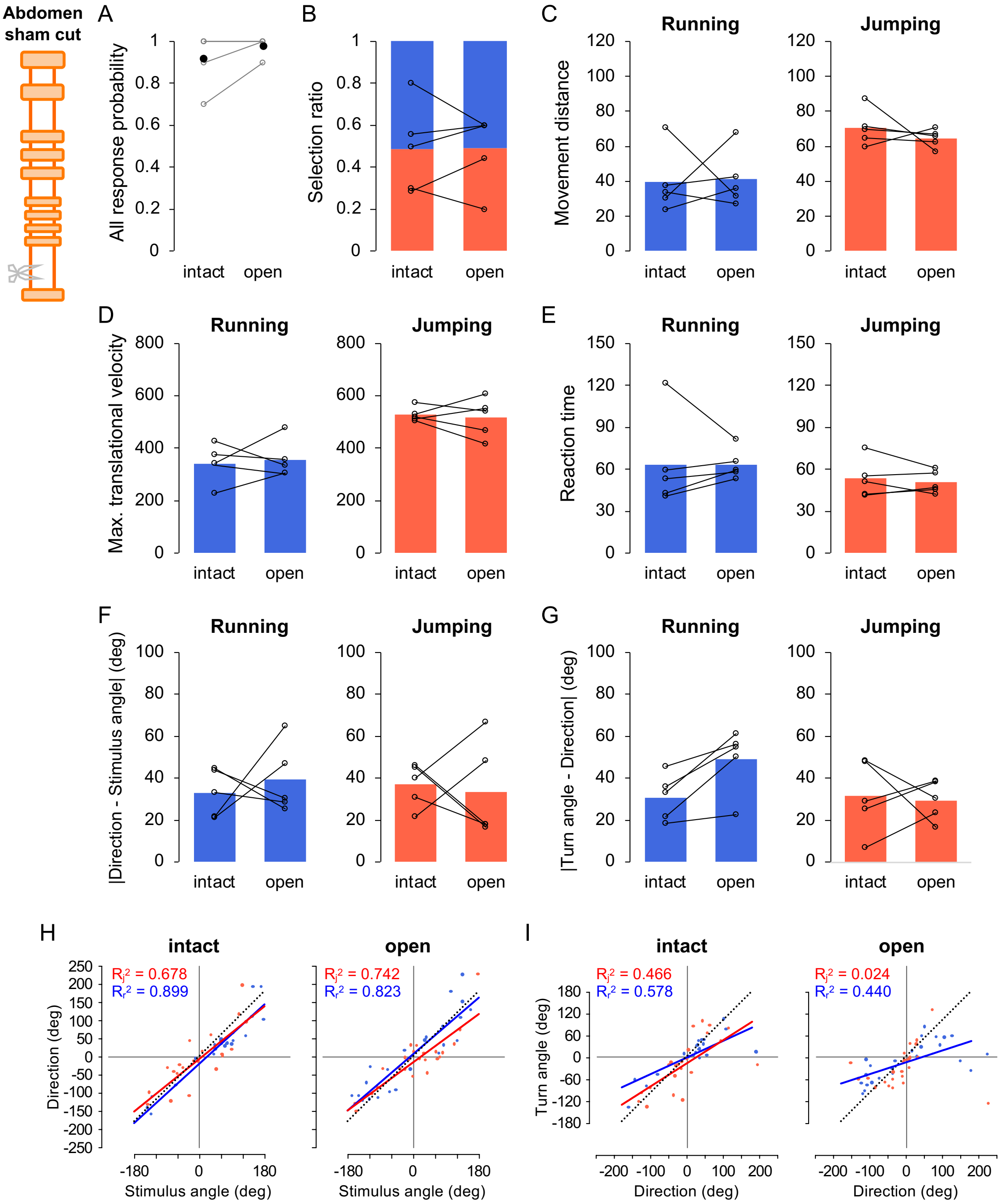

Fig. S3. Sham-surgery of abdomen-cut experiment did not affect the escape behavior. **(A)** All response probability under intact and sham-operated conditions. Gray open circles connected with gray lines represent the response probability for each individual, and black filled circles represent the mean of the probabilities for all individuals. **(B)** Selection ratio of the running (blue) and jumping (red) in all trials under intact and sham-operated conditions. Black lines connect the proportion of the jumping responses per all responding trials for each individual. GLMM indicated that the effect of “$open$” was not significant ($P = 0.931$). **(C–G)** Movement distance (C), maximum translational velocity (D), reaction time (E), absolute values of the difference between the movement direction and stimulus angle (F), and between the turn angle and movement direction (G) under intact and sham-operated conditions. Colored bars indicate the mean value of data in all responding trials of running (blue) or jumping (red). Black open circles connected with lines indicate the mean value of data for each individual. LMM for (C) indicated significant effects of “$response$” ($P < 0.001$), but not of “$open$” ($P = 0.807$) or the interaction of “$response$” and “$open$” ($P = 0.463$). LMM for (D) indicated significant effects of “$response$” ($P < 0.001$), but not of “$open$” ($P = 0.907$) or the interaction of “$response$” and “$open$” ($P = 0.462$). LMM for (E) indicated none of “$response$”, “$open$” and the interaction of “$response$” and “$open$” had significant effect ($P = 0.130$ for “$response$”, $P = 0.870$ for “$open$”, $P = 0.831$ for the interaction of “$response$” and “$open$”). LMM for (F) indicated none of “$response$”, “$open$” and the interaction of “$response$” and “$open$” had significant effect ($P = 0.502$ for “$response$”, $P = 0.441$ for “$open$”, $P = 0.610$ for the interaction of “$response$” and “$open$”). LMM for (G) indicated none of “$response$”, “$open$” and the interaction of “$response$” and “$open$” had significant effect ($P = 0.827$ for “$response$”, $P = 0.237$ for “$open$”, $P = 0.302$ for the interaction of “$response$” and “$open$”). **(H,I)** Relationships between the movement direction and stimulus angle (H) and those between the turn angle and movement direction (I) under intact (left) and sham-operated conditions (right) in running (blue) and jumping (red). Colored lines represent linear regression lines for which significant correlation was observed, and black dotted lines represent $y = x$ lines. $N = 5$ animals.

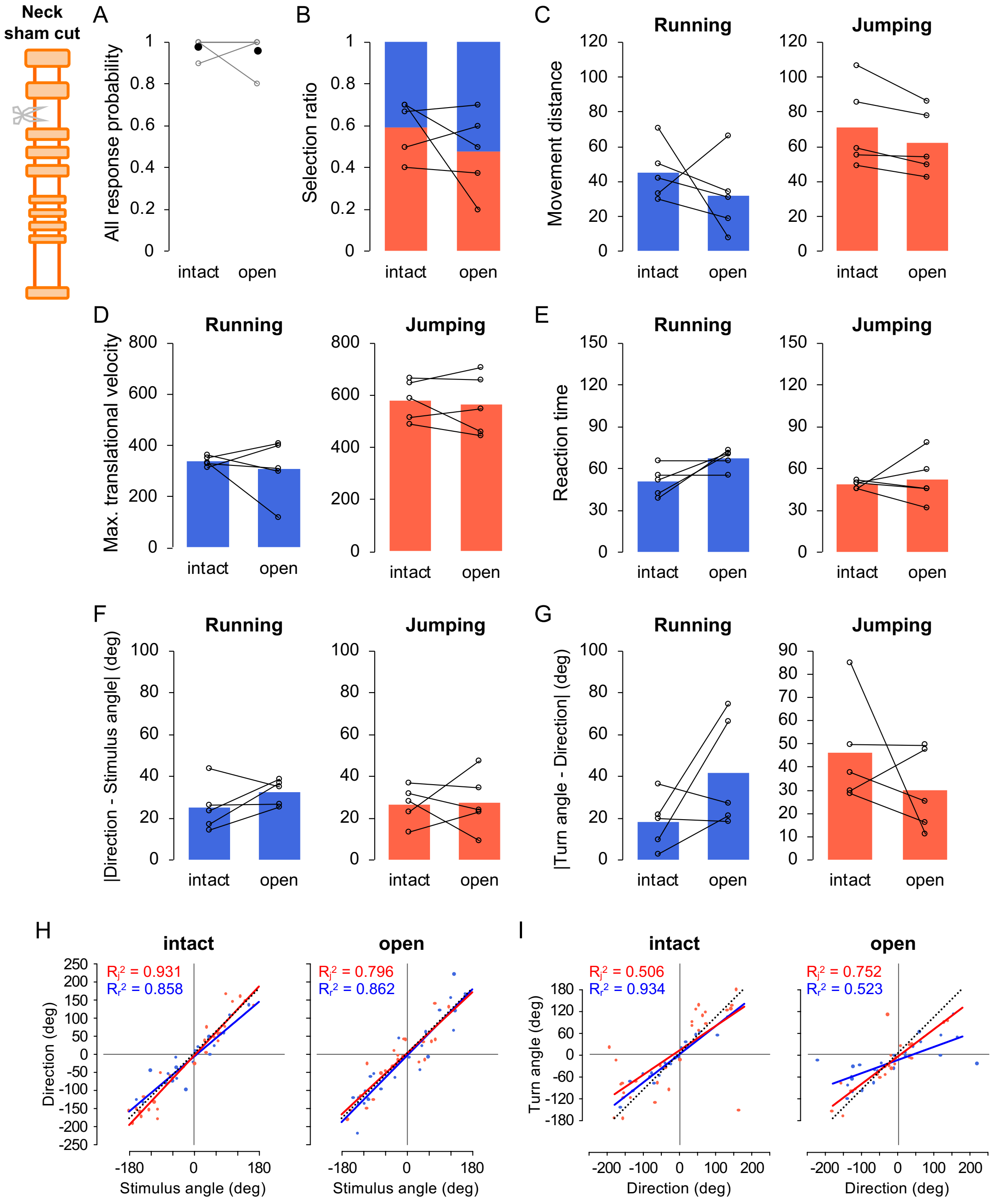

Fig. S4. Sham-surgery of neck-cut experiment had little impacts on the escape behavior. (A) All response probability under intact and sham-operated conditions. Gray open circles connected with gray lines represent the response probability for each individual, and black filled circles represent the mean of the probabilities for all individuals. **(B)** Selection ratio of the running (blue) and jumping (red) in all trials under intact and sham-operated conditions. Black lines connect the proportion of the jumping responses per all responding trials for each individual. GLMM indicated that the effect of "$open$" was not significant (P = 0.267). **(C–G)** Movement distance (C), maximum translational velocity (D), reaction time (E), absolute values of the difference between the movement direction and stimulus angle (F) and between the turn angle and movement direction (G) under intact and sham-operated conditions. Colored bars indicate the mean value of data in all responding trials of running (blue) or jumping (red). Black open circles connected with lines indicate the mean value of data for each individual. LMM for (C) indicated significant effects of "$response$" (P = 0.013) and "$open$" (P = 0.027), but not of the interaction of "$response$" and "$open$" (P = 0.312). LMM for (D) indicated significant effects of "$response$" (P < 0.001), but not of "$open$" (P = 0.328) or the interaction of "$response$" and "$open$" (P = 0.801). LMM for (E) indicated significant effects of "$open$" (P = 0.014), but not of "$response$" (P = 0.820) or the interaction of "$response$" and "$open$" (P = 0.239). LMM for (F) indicated none of "$response$", "$open$" and the interaction of "$response$" and "$open$" had significant effect (P = 0.796 for "$response$", P = 0.185 for "$open$", P = 0.521 for the interaction of "$response$" and "$open$"). LMM for (G) indicated significant effects of "$response$" (P = 0.009), "$open$" (P = 0.005) and the interaction of "$response$" and "$open$" (P = 0.002). **(H,I)** Relationships between the movement direction and stimulus angle (H) and those between the turn angle and movement direction (I) under intact (left) and sham-operated conditions (right) in running (blue) and jumping (red). Colored lines represent linear regression lines for which significant correlation was observed, and black dotted lines represent $y = x$ lines. N = 5 animals.

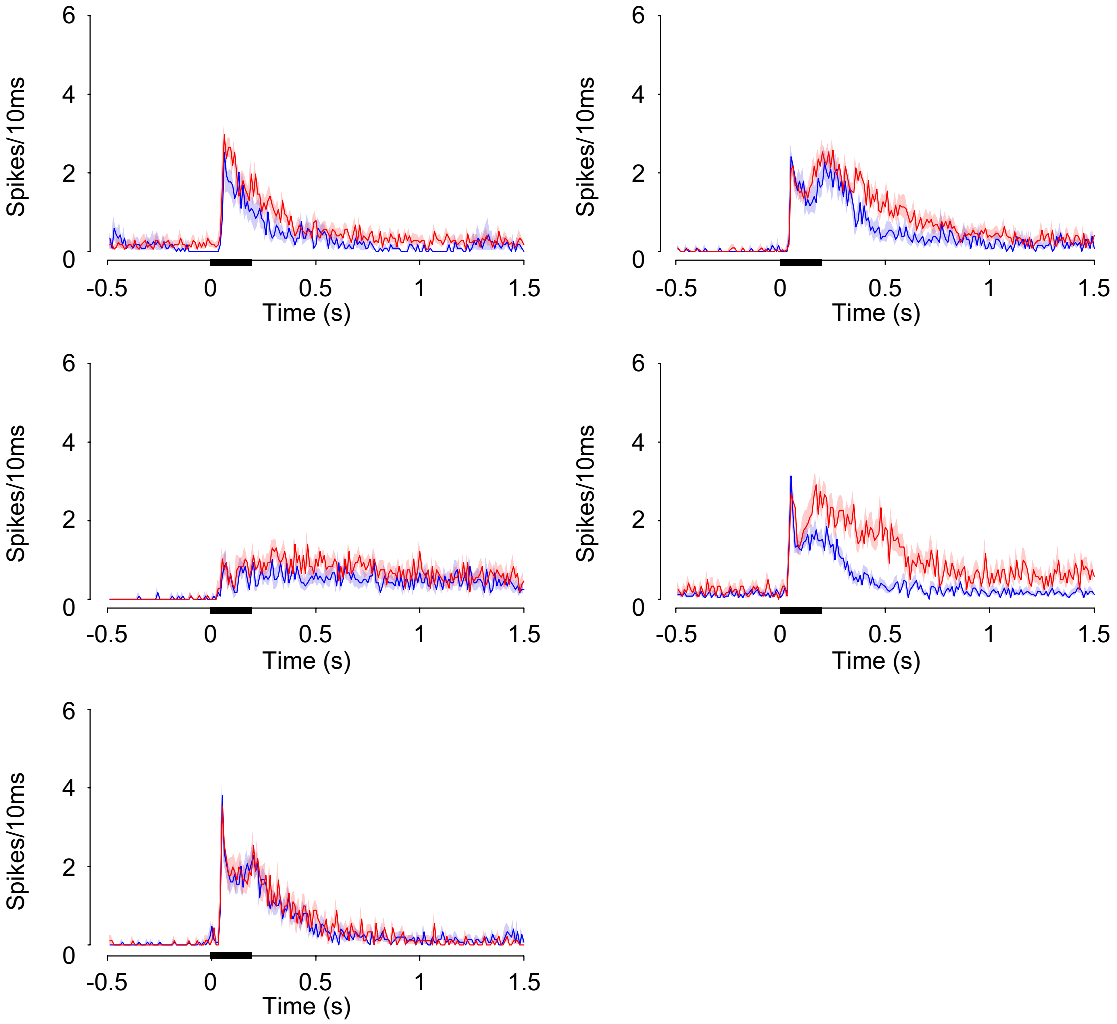

Fig. S5. Time courses in the firing rate of descending spikes during running and jumping. The colored lines indicate the mean of the number of spikes for each 10-ms time-bin in all responding trials of running (blue) and jumping (red) in each individual. The light-colored areas above and below the lines represent the range of mean ± SEM. Black bars indicate the stimulation, of which the onset was indicated as 0 on the time axis. Five panels indicate the data recorded from different individuals, other than those shown in Fig. 8E.

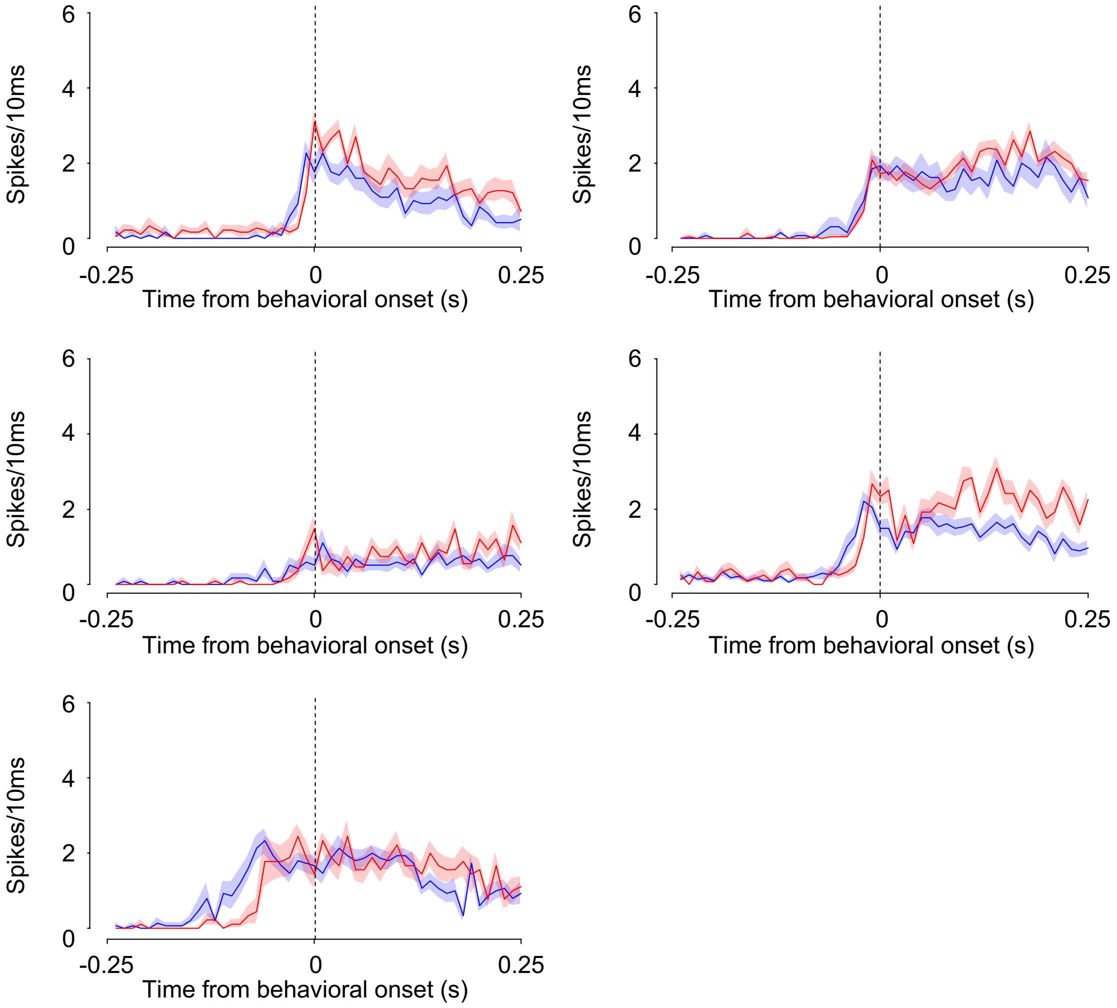

Fig. S6. Time courses in the firing rate of descending spikes in running and jumping aligned with the behavioral onset. The colored lines indicate the mean of the number of spikes for each 10-ms time-bin, which were aligned with the start of leg movement, in all responding trials of running (blue) and jumping (red) in each individual. The light-colored areas above and below the lines represent the range of mean ± SEM. The black dotted lines indicate the behavioral onset, which is also indicated as 0 on the time axes. Five panels indicate the data recorded from different individuals, other than those shown in Fig. 8F.

Supplemental Tables

Table S1. Summary of the number of trials in each type of responses in abdomen-cut and neck-cut experiments.

Abdomen-cut experiment

Condition	Stimulated side	Running	Jumping	No response
Before cutting (intact)	Ipsilateral	97	97	4
	Contralateral	88	110	4
After cutting (ablated)	Ipsilateral	52	11	126
	Contralateral	113	64	34

Neck-cut experiment

Condition	Stimulated side	Running	Jumping	No response
Before cutting (intact)	Ipsilateral	93	105	4
	Contralateral	98	98	2
After cutting (ablated)	Ipsilateral	88	19	84
	Contralateral	116	79	14

Table S2. Summary of the results of GLMM, LMM and linear regression analyses for sham-surgery of abdomen-cut experiment.

GLMM analysis

Parameter	Explanatory variable	Significance of coefficients	
		Z value	p value
All response probability (Fig. S3A)	Open	1.346	0.178
Selection ratio (Fig. S3B)	Open	-0.087	0.931

LMM analysis

Explanatory variable	Significance of coefficients								
	Distance (Fig. S3C)			Velocity (Fig. S3D)			Reaction time (Fig. S3E)		
	df	t	p	df	t	p	df	t	p
response	87	4.859	<0.001	87	5.747	<0.001	87	-1.529	0.130
open	87	-0.245	0.807	87	0.118	0.907	87	-0.164	0.870
response:open	87	-0.737	0.463	87	-0.739	0.462	87	-0.214	0.831

LMM analysis

Explanatory variable	Significance of coefficients					
	Difference between direction and stimulus angle (Fig. S3F)			Difference between turn angle and direction (Fig. S3G)		
	df	t value	p value	df	t value	p value
response	87	0.674	0.502	87	0.220	0.827
open	87	0.774	0.441	87	1.190	0.237
response:open	87	-0.512	0.610	87	-1.039	0.302

Linear regression analysis

Parameter	Condition	Response	Result of linear regression		
			Estimated slope	t value	p value
Direction against stimulus angle (Fig. S3H)	Intact	Running	0.904	13.64	<0.001
		Jumping	0.806	6.652	<0.001
	Open	Running	0.862	10.36	<0.001
		Jumping	0.741	7.948	<0.001
Turn angle against direction (Fig. S3I)	Intact	Running	0.458	5.360	<0.001
		Jumping	0.630	4.279	<0.001
	Open	Running	0.330	4.247	<0.001
		Jumping	0.116	0.734	0.471

Supplemental Table S3. Summary of the results of GLMM, LMM and linear regression analyses for sham-operation of neck-cut experiment.

GLMM analysis

Parameter	Explanatory variable	Significance of coefficients	
		Z value	p value
All response probability (Fig. S4A)	Open	-0.577	0.564
Selection ratio (Fig. S4B)	Open	-1.110	0.267

LMM analysis

Explanatory variable	Significance of coefficients								
	Distance (Fig. S4C)			Velocity (Fig. S4D)			Reaction time (Fig. S4E)		
	df	t	p	df	t	p	df	t	p
response	89	2.527	0.013	89	5.931	<0.001	89	-0.228	0.820
open	89	-2.251	0.027	89	-0.984	0.328	89	2.497	0.014
response:open	89	1.016	0.312	89	-0.253	0.801	89	-1.184	0.239

LMM analysis

Explanatory variable	Significance of coefficients					
	Difference between direction and stimulus angle (Fig. S3F)			Difference between turn angle and direction (Fig. S3G)		
	df	t value	p value	df	t value	p value
response	89	0.259	0.796	89	2.660	0.009
open	89	1.337	0.185	89	2.902	0.005
response:open	89	-0.645	0.521	89	-3.147	0.002

Linear regression analysis

Parameter	Condition	Response	Result of linear regression		
			Estimated slope	t value	p value
Direction against stimulus angle (Fig. S4H)	Intact	Running	0.842	10.43	<0.001
		Jumping	1.062	19.06	<0.001
	Open	Running	1.025	11.98	<0.001
		Jumping	0.940	9.046	<0.001
Turn angle against direction (Fig. S4I)	Intact	Running	0.772	15.89	<0.001
		Jumping	0.672	5.263	<0.001
	Open	Running	0.360	5.021	<0.001
		Jumping	0.756	7.988	<0.001

Supplemental Table S4. Summary of the results of GLMM analyses for response probability in abdomen-cut and neck-cut experiments.

Abdomen-cut experiment

Parameter	Explanatory variable	Significance of coefficients	
		Z value	p value
All response probability (Fig. 2D)	cut	-4.315	<0.001
	side	-0.055	0.956
	cut:side	-3.371	<0.001
Selection ratio (Fig. 2H)	cut	-3.736	<0.001
	side	-1.104	0.269
	cut:side	-1.826	0.068

Neck-cut experiment

Parameter	Explanatory variable	Significance of coefficients	
		Z value	p value
All response probability (Fig. 3D)	cut	-2.596	<0.001
	side	-0.883	0.377
	cut:side	-2.095	0.036
Selection ratio (Fig. 3H)	cut	-1.843	0.065
	side	0.644	0.520
	cut:side	-3.820	<0.001

Supplemental Table S5. Summary of the results of LMM analyses for probability change in abdomen-cut and neck-cut experiments.

Abdomen-cut experiment

Parameter	Explanatory variable	Significance of coefficients		
		df	t value	p value
Probability change (Fig. 2G)	response	57	-4.933	<0.001
	side	57	-5.083	<0.001
	response:side	57	1.576	0.121

Neck-cut experiment

Parameter	Explanatory variable	Significance of coefficients		
		df	t value	p value
Probability change (Fig. 3G)	response	57	-1.536	0.130
	side	57	-0.331	0.742
	response:side	57	-2.781	0.007

Supplemental Table S6. Summary of the results of LMM analyses for locomotor parameters in abdomen-cut and neck-cut experiments.

Abdomen-cut experiment

Explanatory variable	Significance of coefficients								
	Distance (Fig. 4A)			Velocity (Fig. 4B)			Reaction time (Fig. 4C)		
	df	t	p	df	t	p	df	t	p
response	605	6.841	<0.001	605	12.01	<0.001	605	-0.496	0.620
cut	605	-4.243	<0.001	605	-3.855	<0.001	605	3.105	0.002
side	605	0.924	0.356	605	0.060	0.952	605	-1.619	0.106
response:cut	605	1.039	0.299	605	0.212	0.832	605	-1.406	0.160
response:side	605	-0.610	0.542	605	0.251	0.802	605	0.774	0.439
cut:side	605	-2.508	0.012	605	-2.082	0.038	605	5.688	<0.001
response:cut:side	605	-0.050	0.960	605	0.618	0.537	605	-1.400	0.162

Neck-cut experiment

Explanatory variable	Significance of coefficients								
	Distance (Fig. 5A)			Velocity (Fig. 5B)			Reaction time (Fig. 5C)		
	df	t	p	df	t	p	df	t	p
response	669	9.555	<0.001	669	13.13	<0.001	669	-0.502	0.616
cut	669	-7.199	<0.001	669	-10.01	<0.001	669	0.399	0.690
side	669	-0.263	0.793	669	0.488	0.626	669	1.220	0.223
response:cut	669	1.438	0.151	669	2.733	0.006	669	-1.503	0.133
response:side	669	0.050	0.960	669	-0.164	0.870	669	-0.410	0.682
cut:side	669	-1.169	0.243	669	-1.819	0.069	669	2.785	0.006
response:cut:side	669	0.327	0.744	669	0.824	0.410	669	0.044	0.965

Supplemental Table S7. Summary of the results of LMM analyses for differences in locomotor parameters.

Explanatory variable	Significance of coefficients								
	Distance (Fig. S2A)			Velocity (Fig. S2B)			Reaction time (Fig. S2C)		
	df	t	p	df	t	p	df	t	p
response	109	1.949	0.054	109	1.286	0.201	109	-0.858	0.393
side	109	-1.696	0.093	109	-1.847	0.068	109	4.938	<0.001
location	109	-3.000	0.003	109	-4.584	<0.001	109	-1.291	0.200
response:side	109	-0.478	0.634	109	0.667	0.506	109	-1.738	0.085
response:location	109	0.996	0.322	109	1.922	0.057	109	0.049	0.961
side:location	109	0.170	0.866	109	0.142	0.887	109	-2.061	0.042
response:side: location	109	1.332	0.186	109	0.898	0.371	109	1.018	0.311

Supplemental Table S8. Summary of the result of linear regression analyses for the directional control of the escape movements in abdomen-cut and neck-cut experiments.

Abdomen-cut experiment

Parameter	Condition	Response	Result of linear regression		
			Estimated slope	t value	p value
Direction against stimulus angle (Fig. 6A)	Intact	Running	1.026	47.76	<0.001
		Jumping	1.003	41.80	<0.001
	Ablated	Running	1.028	30.10	<0.001
		Jumping	0.894	14.40	<0.001
Turn angle against direction (Fig. 6B)	Intact	Running	0.598	16.68	<0.001
		Jumping	0.395	6.373	<0.001
	Ablated	Running	0.038	1.318	0.189
		Jumping	0.028	0.274	0.785

Neck-cut experiment

Parameter	Condition	Response	Result of linear regression		
			Estimated slope	t value	p value
Direction against stimulus angle (Fig. 7A)	Intact	Running	0.897	36.57	<0.001
		Jumping	1.015	38.80	<0.001
	Ablated	Running	0.858	23.09	<0.001
		Jumping	0.846	8.228	<0.001
Turn angle against direction (Fig. 7B)	Intact	Running	0.557	15.77	<0.001
		Jumping	0.440	7.462	<0.001
	Ablated	Running	0.006	0.342	0.733
		Jumping	0.046	0.551	0.583

Supplemental Table S9. Summary of the result of LMM analyses for absolute difference between angular parameters in abdomen-cut and neck-cut experiments.

Abdomen-cut experiment

Explanatory variable	Significance of coefficients					
	Difference between direction and stimulus angle (Fig. 6C)			Difference between turn angle and direction (Fig. 6D)		
	df	t value	p value	df	t value	p value
response	605	2.129	0.034	605	2.985	0.003
cut	605	2.455	0.014	605	0.576	0.565
side	605	0.369	0.712	605	0.625	0.532
response:cut	605	-1.911	0.057	605	-1.640	0.102
response:side	605	-1.593	0.112	605	-0.784	0.434
cut:side	605	4.168	<0.001	605	6.146	<0.001
response:cut:side	605	1.055	0.292	605	0.961	0.337

Neck-cut experiment

Explanatory variable	Significance of coefficients					
	Difference between direction and stimulus angle (Fig. 7C)			Difference between turn angle and direction (Fig. 7D)		
	df	t value	p value	df	t value	p value
response	669	-0.932	0.352	669	2.684	0.007
cut	669	6.048	<0.001	669	1.856	0.064
side	669	0.100	0.920	669	-0.156	0.876
response:cut	669	1.825	0.068	669	-0.928	0.354
response:side	669	1.101	0.271	669	-0.105	0.916
cut:side	669	-0.201	0.841	669	1.553	0.121
response:cut:side	669	-3.710	<0.001	669	-1.933	0.054

Supplemental Table S10. Summary of the number of recordings in each types of response in electrophysiological experiments.

Individuals	Running	Jumping
ID081901	12	18
ID092002	12	11
ID092302	25	7
ID102302	13	22
ID101504	25	12
ID102302	15	9

Supplemental Table S11. Summary of the result of likelihood ratio tests for LMMs for the extracellular recording data.

Parameter	Result of likelihood ratio test	
	Chi-squared	p value
First spike timing after stimulus onset (Fig. 8G, left)	2.365	0.124
First spike timing after behavioral onset (Fig. 8G, right)	18.55	<0.001
Total spike count during Pre time (Fig. 8H, left)	9.526	0.002
Total spike count during Post time (Fig. 8H, right)	66.05	<0.001
Spike count during -10~0 ms (Fig. 8I)	11.94	<0.001
Max. spike count during Post time (Fig. 8J)	4.087	0.043

Supplemental Videos

Video S1. High-speed video movie of the typical running response to air-puff stimulus. Airflow was applied from upper side of the image. Red and Green traces indicate the movements of markers pained on the cricket head and thorax, respectively.

Video S2. High-speed video movie of the typical jumping response to air-puff stimulus. Airflow was applied from upper side of the image. Red and Green traces indicate the movements of markers pained on the cricket head and thorax, respectively.